



**Clean Propulsion  
Technologies**

# **Clean Propulsion Technologies, VTT's final report**

Authors: Lehtoranta Kati, Aakko-Saksa Päivi, Söderena Petri, Tuominen Tino, Westerholm Mårten

Confidentiality: VTT Public

Version: 26.4.2024

<b>Report's title</b> Clean Propulsion Technologies, VTT's final report	
<b>Customer, contact person, address</b>	<b>Order reference</b>
<b>Project name</b> Clean Propulsion Technologies	<b>Project number/Short name</b> CPT
<b>Author(s)</b> Lehtoranta Kati, Aakko-Saksa Päivi, Söderena Petri, Tuominen Tino, Westerholm Märten	<b>Pages</b> 39
<b>Keywords</b> Emissions, engines, aftertreatment, hydrogen	<b>Report identification code</b> VTT-R-00278-24
<p><b>Summary</b></p> <p>In the CPT project, VTT had two main tasks to lead. First task focused on advanced aftertreatment technologies and the second focused on variable valve actuation technologies and on studying the performance and potentiality of hydrogen fuelled internal combustion engines. Advanced aftertreatment technologies are needed to supplement the new combustion methodology in order to obtain the ultra-low emission levels. Experimental work, conducted at research facility developed by VTT, concentrated on aftertreatment devices to reach ultralow NO<sub>x</sub> and low particle emissions. All these aftertreatment and emission related experimental studies were closely linked to the company projects proving them valuable information needed in developing technologies to reduce emissions.</p> <p>Variable valve actuation (VVA) technologies, which were studied in the second task lead by VTT, are seen as enablers for achieving the ultra-low emissions. VVA technology enables exhaust gas aftertreatment system operation on optimum operation area allowing low emissions and reduces fuel consumption. Hydrogen combustion in off-road HD engine was studied at VTT as well. Hydrogen is one of the most interested fuel option for the future not only for usage in fuel cells but also in internal combustion engines (ICE). Hydrogen usage in ICE would allow the usage of current vehicle construction without major modifications as the engine itself by its characteristics is similar as current diesels. The hydrogen engine demo produced new relevant knowledge to be used in the companies' own R&amp;D activities.</p>	
<b>Confidentiality</b>	VTT Public
Espoo 26.4.2024 <b>Written by</b>  Kati Lehtoranta, Principal Scientist	<b>Reviewed by</b>  Rasmus Pettinen Senior Scientist
<b>VTT's contact address</b>	
<b>Distribution (customer and VTT)</b> CPT project partners and Business Finland, in addition distribution through VTT's publication database.	
<i>The use of the name of "VTT" in advertising or publishing of a part of this report is only permissible with written authorisation from VTT Technical Research Centre of Finland Ltd.</i>	

## Contents

---

1. Introduction.....	3
2. Description and objectives.....	3
2.1 Task 3.4 ‘Advanced Aftertreatment’ .....	3
2.2 Task 3.7 ‘Advanced high-speed engine’ .....	4
3. Targeting to ultralow NO <sub>x</sub> and avoiding catalyst deterioration .....	6
3.1 Target.....	6
3.2 Methods .....	7
3.3 Results .....	9
3.3.1 NO <sub>x</sub> and NH <sub>3</sub> emissions.....	9
3.3.2 Urea vs ammonia.....	12
3.3.3 Other emissions.....	12
3.4 Main findings .....	14
4. Targeting to low PM.....	15
4.1 Target.....	15
4.2 Methods .....	15
4.2.1 Ash generator.....	15
4.2.2 Doping engine fuel with high ash lubricant.....	16
4.2.3 High ash lubricant injection to intake air.....	17
4.2.4 Test setup and emission measurements.....	18
4.3 Results .....	19
4.3.1 Ash generator study.....	19
4.3.2 High ash lubricant injection to intake air.....	22
4.3.3 Doping engine fuel with high ash lubricant.....	24
Main findings .....	25
5. Ultralow NO <sub>x</sub> EAT Thermal management.....	25
5.1 Target.....	25
5.2 Methods .....	25
5.3 Results .....	26
5.4 Main findings .....	30
6. Towards Hydrogen-fuelled engine demonstrator .....	30
6.1 Target.....	30
6.2 Methods .....	31
6.3 Results .....	34
6.4 Main findings .....	38
References .....	39

## 1. Introduction

---

Both climatic and health effects are associated to engine emissions. In this project, the focus is on marine and off-road sectors – which face different requirements by different emission regulations. At the same time both sectors face the necessity to drastically cut down the CO<sub>2</sub> footprint. The rapidly changing situation forces a major shift in the current roadmap for marine and off-road propulsion technologies towards exploring more sustainable solutions. While the combustion engine is expected to remain the prime mover in these sectors due to large energy density requirements, it will require new solutions in terms of both the fuel and the combustion technology. Furthermore, securing efficient and clean energy conversion will require the development of various hybrid technologies.

Considering forthcoming changes in marine and off-road segments, the goal of the Clean Propulsion Technologies Consortium is to secure global technology leader position for the Finnish powertrain industry by creating common vision and sustainable business solutions.

New exhaust gas aftertreatment devices, combustion methods and renewable fuels enabling close to zero tailpipe emissions even in the most challenging engine operation conditions are needed to secure clean air for the people, to reduce CO<sub>2</sub> footprint and to improve energy efficiency. The VTT subprojects are focusing on these core research questions by studying new sophisticated high efficiency aftertreatment technologies and variable valve actuation technologies which enables the close to zero tailpipe emissions and lower fuel consumption. First studies of hydrogen as an internal combustion engine fuel gives important information of its potentiality for off-road engine applications.

The VTT subproject thus contributes to the common CPT plan mainly by studies related to combining engine and aftertreatment measures to demonstrate GHG reduction with ultra-low NO<sub>x</sub> and PM emissions and demonstrators of advanced propulsion systems with e.g., hydrogen-fuelled engine demonstrator.

## 2. Description and objectives

---

In the CPT project, VTT works mainly on WP3 'Novel combustion concepts and advanced aftertreatment solutions' that aims to provide a significant progress along both - the novel combustion concepts roadmap and advanced aftertreatment theme. Two tasks in WP3, namely Task 3.4 'Advanced Aftertreatment' and Task .3.7 'Advanced high-speed engine' are led by VTT.

### 2.1 Task 3.4 'Advanced Aftertreatment'

By developing advanced aftertreatment systems the project targets to reach near zero levels of pollutants (NO<sub>x</sub> and particles) minimizing also the negative effects of those pollutants. In this project, the focus is on marine and off-road sectors – which face different requirements by different emission regulations, and therefore, aftertreatment systems for these sectors are at different stages of development. The advantage of this project is it brings these sectors together making it easy to learn from the other sector. The task utilizes different experimental environments of VTT. Within this task three comprehensive experimental campaigns are conducted at VTT facilities. The task is further divided to subtasks:

#### T.3.4.1 Targeting to ultralow NO<sub>x</sub> and avoiding catalyst deterioration

Together with the company projects of Dinex and AGCO, this subtask studies possible new as well as known catalysts and their combinations to find the best candidates to reach near zero NO<sub>x</sub> levels. This

subtask combines knowledge of experts and state-of-the-art techniques; including techniques developed in companies own projects, into the same experiments.

- First the research facility developed at VTT especially for after-treatment and emission studies is modified to be suitable to study the advanced after-treatment systems of this project. The engine parameter setup and operating points will be selected to meet the real-life application reference values. Primarily, steady state experiments are relevant in catalyst developments. Readiness for installations of different catalyst and filter combinations is enabled.
- Techniques developed by engine and catalyst manufacturers in companies' own projects will be studied utilizing the research facility with the possibilities to adjust the exhaust gas composition, flow and temperature. Within the scope of this research project, a couple of most promising techniques (e.g. after-treatment systems) are studied. One system is Double-SCR, when the focus of experimental studies would be in the first SCR unit specifically. In addition, the other possible catalysts and/or filter involved are included in the study as well as the injection and mixing systems of ammonia or urea involved in SCR systems, since they are in important role in ensuring all the injected ammonia be utilized as effectively as possible for the NO<sub>x</sub> reduction.
- As comprehensive emission characterization as possible is needed to produce information for development of new catalysts. In addition to NO<sub>x</sub>, other important gaseous emissions are measured, like NH<sub>3</sub>, N<sub>2</sub>O, CO, CO<sub>2</sub> and hydrocarbons. To have an overall picture, particle emission studies are included in part of the experiments, as well.

#### T.3.4.2 Targeting to low PM

How to reach maximum particle emission reduction with aftertreatment? Particle filters (PF) are well-known devices e.g., in vehicles to effectively decrease particle emissions. These filters as such cannot be directly applied to ships, e.g., due to implementation of low quality fuels on the marine sector. However, in the near future, more and more ships will need aftertreatment technologies to reduce particle emissions, since both climatic and health effects are associated to particle emissions of ships. This task, together with the company projects of Wärtsilä and Dinex, studies different PF's and alternative solutions to reduce both particle mass (PM) (including black carbon) and particle number (PN) emissions.

- High-speed engine and VTT's test bench are involved in the first phase studies.
- Fuel and lubricant compositions are important to filter operation, and those are to be carefully selected in cooperation with companies involved. In addition, the possible catalyst (e.g., SCR) involved might have significant effect on filter performance and is included in part of the studies.
- Particle emission measurements are in key role, meaning PM, PN, black carbon (BC) and PM composition while gaseous emission studies are included as well.

#### Task 3.4.3 RCCI combustion & emission control

At the end of the project, the first RCCI medium-speed demo was planned to be conducted at VEBIC in Vaasa. To study the exhaust gas composition comprehensively during the demo, VTT's and UVA's expertise and equipment were planned to be combined. These plans will not be included in this VTT's report as they are part a separate report led by UVA, while VTT contributed to it.

## 2.2 Task 3.7 'Advanced high-speed engine'

T3.7 tackles the short-term issues relevant for high-speed engines used in off-road applications. This involves incorporation of advanced variable valve actuation technology for thermal management (3.7.1-

2) and a first demonstrator of combustion engine application running 100% on Hydrogen (3.7.3). This at the same time complements the long term vision of marine propulsion development and creates a clear binding point between T.3.3 (variable valve actuation instrumental in T3.7 also used as an enabler for RCCI in T3.3) and T3.4 (the thermal management contributes to realizing targets on aftertreatment side).

Ultra-low NO<sub>x</sub> and PM emissions can be achieved with sophisticated combustion, aftertreatment methods and fuels. However, aftertreatment systems require high exhaust gas temperature to achieve high emissions reduction rate. For this purpose, sophisticated valve control methods provide a tool for reducing the mass of combustion air or even shutting some of the cylinders during the operation. These methods provide the potential for increasing the exhaust gas enthalpy and simultaneously reducing the fuel consumption. In this project, these methods are studied with simulations and experimental work on engine dyno with unique research engine that is equipped with variable valve actuation system. In addition, the potential of hydrogen as high-speed heavy-duty off-road engine fuel is studied.

Actions taken in tasks:

#### T3.7.1 Ultralow NO<sub>x</sub> EAT Thermal management

VTT will design in cooperation with AGCO Power a state-of-the-art test engine that have fully variable valve train. Current heavy-duty engines (on-road and off-road) do not include variable valve actuation (VVA) systems. This technology will open totally new opportunities for reducing emissions and fuel consumption. Up to date, more and more stringent emission limits have had negative effect on improvements in fuel economy as sophisticated exhaust aftertreatment devices requires high exhaust gas temperature. Variable valve actuation studied in this task could potentially give up to 5 to 10 % reduction in fuel consumption. This will be also one of the targets for the task.

AGCO Power four-cylinder Stage V diesel engine will be used as a base engine. Cylinder head will be modified so that new valve train with fully variable valve lift and timing is possible to achieve. VTT and AGCO Power will design the system together with the support of third company focused on variable valvetrains. New type of test engine gives the possibility to study different engine internal strategies, which increase exhaust gas temperature without deteriorating fuel economy. Such strategies include:

- cylinder cut-off (shutting down of part of the cylinders)
- early intake valve closing and late intake valve closing
- internal exhaust recirculation with exhaust valve opening during the intake stroke
- reduced intake valve lift
- mixture of above mentioned methods

Below are listed the main objectives for the testing:

- Study the potentiality of different VVA strategies in question of exhaust gas temperature, engine transient capabilities and fuel economy
- Find a VVA strategy that enables high NO<sub>x</sub> emissions reduction with sophisticated SCR systems on low engine loading areas and simultaneously improve fuel consumption by 5 - 10 %
- Get first experience of capabilities and possible restrictions of VVA strategies for HD non-road engine purposes

The test engine will be equipped with engine control system that allows VTT fully control the engine operation. VTT's high-speed engine test facility will be used for the test program.

### T3.7.3 Towards Hydrogen-fuelled engine demonstrator

Due to its carbon free composition, hydrogen is not only interesting fuel for fuel cell applications, but also for internal combustion engines. Hydrogen fuelled internal combustion engines have the advantage over fuel cells because the technology is nearly comparable with the current technologies, and thus are close to fully compatible with the existing heavy-duty vehicle design. Furthermore, hydrogen engines are less expensive than fuel cells.

Because hydrogen fuel is carbon-free, it opens opportunities to reduce costly exhaust aftertreatment system as no carbon based emissions are emitted, such as HC, CO, PM emissions. In addition, hydrogen with good flammability and high flame speed opens up possibility for new combustion strategies such as lean burn concept that is not possible for traditional spark-ignited engines. These strategies enables to achieve lower flame temperature and thus lower NO<sub>x</sub> emissions and at the same time, thanks to hydrogen good combustion characteristics, high efficiency.

VTT will build in a cooperation with AGCO Power a new spark-ignited test engine that utilize hydrogen as a fuel. Engine will be equipped with hydrogen direct injection and specially designed combustion related components such as piston bowl, compression ratio, intake manifold and ports.

Objectives for testing are:

- Obtain first experiences of hydrogen combustion and its potentiality
- Perform measurements on EU Stage V Non-Road Steady Cycle (NRSC) and other steady test points and compare results against Stage V legislation
- Study the performance and boundaries of hydrogen fuelled engine
- Formulate understanding and deepen the knowledge of the special characteristics that hydrogen requires from internal combustion engine in construction and control wise
- Formulate an understanding of possibly required exhaust gas aftertreatment system

VTT's high-speed engine test facility will be used for the test program. Test facility will be equipped with the special safety instruments required for hydrogen.

In addition to above described tasks, VTT is strongly involved in dissemination, reporting and publishing the project results. In addition to normal project reporting, the results will be published as scientific papers in peer review journals as well as in conferences. Open access publications will be favoured.

## 3. Targeting to ultralow NO<sub>x</sub> and avoiding catalyst deterioration

---

### 3.1 Target

In order to meet even stringent emission limits in future (e.g., Euro 7 emission standards under discussion in Europe), aftertreatment systems need further development. There are also operation conditions where the current aftertreatment technology is not good enough in reducing the emission levels. These include, for example, conditions where the exhaust gas temperature is low. The future NO<sub>x</sub> emission regulations have resulted in various proposals to apply thermal management (i.e., electric heating), SCR on filter (FSCR), passive NO<sub>x</sub> adsorption (PNA) and double SCR, where a closed-coupled (CC) SCR catalyst is installed before large DOC+DPF in the system [Harris et al. 2019, Kasab et al. 2021]. This smaller CC-SCR catalyst is utilizing the higher exhaust gas temperatures after engine in

warm-up and continuous low temperature drive. However, when the space before DOC+DPF is limited and the additional SCR unit limits DOC operation and PM regeneration (lower temperatures), a smaller SCR catalyst volume is necessary.

In present study targeting to decrease the  $\text{NO}_x$  further from a heavy-duty engine in all operation conditions we introduce a double-SCR system. This double-SCR system would involve two different SCR units, one placed upstream the DPF and another placed downstream of the DPF. In this study, we investigate three CC-SCR catalysts and their performance upstream of the DPF, at different exhaust temperatures.

## 3.2 Methods

Planning of the experiments was done in close co-operation with VTT, AGCO and Dinex.

The engine for the studies was provided by the project partner AGCO. It was an AGCO Power 44 HD Stage V engine with four cylinders, displacement of 4,4 liters, with a maximum power of 111 kW (at 1800 rpm) and a maximum torque of 650 Nm (at 1500 rpm). EN590 diesel fuel was utilized in all tests.

Three different catalysts were studied: a vanadium-based SCR (V-SCR), a copper-based SCR (Cu-SCR) and a vanadium-based SCR including a Pt containing ammonia slip catalyst (V-SCR+ASC). The SCR-catalyst size was 1,4 liters in all three cases. So also, the V-SCR+ASC and V-SCR having similar SCR-part, had the same total volume meaning that in the V-SCR+ASC approximately 20% of the SCR-catalyst volume was replaced by the ammonia slip catalyst. All catalysts were provided by project partner Dinex.

All SCR catalysts were preconditioned in air for four hours at 600 °C prior to the actual experiments.

Aqueous 32.5% urea solution was used in the experiments. In order to have the urea well decomposed into ammonia before entering the catalyst, a mixer was used upstream the SCR. This urea solution mixer used in the test was adapted from a non-road Stage V exhaust line.

The studies were started with short experiments at different urea feeds i.e.,  $\text{NH}_3/\text{NO}_x$  ratios, starting from approximately 0.3 to above 1. Based on these pre-experiments, few  $\text{NH}_3/\text{NO}_x$  ratios were selected to study further. Since the CC-SCR does not target to maximum  $\text{NO}_x$  reduction at all conditions, but to help the following SCR unit, both,  $\text{NH}_3/\text{NO}_x$  ratio well below one as well as a high ratio close to one were studied. These  $\text{NH}_3/\text{NO}_x$  ratios were 0.5 and 1.05.

In addition, to achieve even better  $\text{NO}_x$  reduction, ammonia gas was used instead of urea to understand if the SCR could really perform better with ammonia. In this case, a gas bottle with 10% ammonia gas in nitrogen was utilized as a source of ammonia.

In addition to the SCR unit, a diesel oxidation catalyst (DOC) and diesel particulate filter (DPF) combination followed the SCR (see Figure 1). The DOC+DPF was kept the same, although the SCR unit was changed during the experiments.



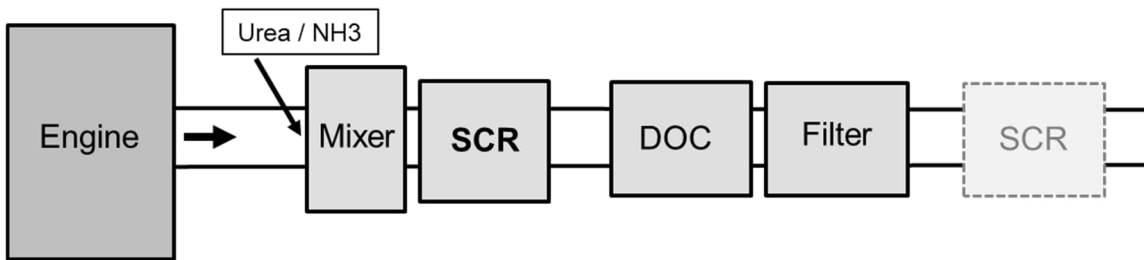


Figure 1 Simplified description of the setup for catalyst experiments.

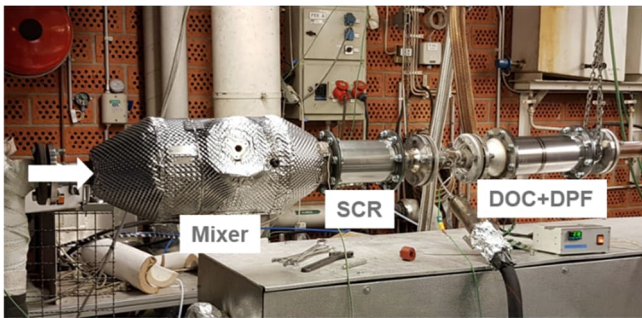


Figure 2 Photo of the catalysts' setup.

The basics of the research facility was presented in detail in Murtonen et al. 2016. The exhaust gas flow and temperature (measured upstream of the catalysts) were adjusted independently when only a part of exhaust was conducted into the catalyst reactor and therefore it was possible to keep feed conditions constant even when changing the engine driving mode. All experiments were conducted at steady state driving modes. In these modes engine out  $\text{NO}_x$  levels were approx. 750 ppm or 1000 ppm (see Table 1). Exhaust temperatures utilized in studies were 215, 250, 280 and 350 °C. Exhaust gas flow was kept constant at 100 kg/h in all tests. This results to space velocities (SV) in the order of 100 000 h<sup>-1</sup> for the SCR units.

Table 1 Conditions for experiments.

Exhaust flow (kg/h)	100	100	100	100
Exhaust T (°C)	215	250	280	350
Engine out $\text{NO}_x$ (ppm)	750	1000	1000	750
SV of SCR (1/h)	99 000	106 000	112 000	126 000

Emission measurements were conducted from different points; as engine out (i.e., upstream of the SCR), downstream of the SCR (i.e., upstream of the DOC) and downstream of the DOC+DPF (see Figure 1). The emission measurement setup consisted of a chemiluminescence detector (CLD), used to measure the  $\text{NO}_x$  ( $\text{NO}$ ,  $\text{NO}_2$ ) and a non-dispersive infrared (NDIR) analyser to measure CO and  $\text{CO}_2$ . An FTIR (Fourier transform infrared spectroscopy) analyser was also used to measure  $\text{NO}_x$  and CO, as well as many other components, like water and  $\text{NH}_3$  concentrations. The FTIR as well as the sampling line and the filter prior to the FTIR spectrometer were heated to 180 °C.

In a part of the experiments, also particle emissions were studied. Particulate matter (PM) was studied by sampling PM both 'engine out' and 'after the DOC+DPF' with a sampling according to international standard ISO 8178. According to this standard the PM is measured as any material collected on a filter

after diluting exhaust gas with clean, filtered air to a temperature higher than 42 °C and less than or equal to 52 °C, as measured at a point immediately upstream of the filter. A dilution ratio of 10 was used. Samples were collected on TX40HI20-WW filters (Ø 47 mm). The PN measurement method used in this study considers only nonvolatile particles with a diameter greater than 23 nm. Dekati Engine Exhaust Diluter (DEED) was used for PN sample conditioning in the current study. The system consists of two ejector diluters, providing a total dilution ratio of 100:1. The temperature of the first ejector was ~200 °C, and the temperature at the outlet of the DEED unit was below 35 °C. PN>23nm concentrations were determined with an Airmodus A23 Condensation Particle Counter (CPC).

### 3.3 Results

#### 3.3.1 NO<sub>x</sub> and NH<sub>3</sub> emissions

The experiments started with short steady state experiments at different urea feeds (from approx. NH<sub>3</sub>/NO<sub>x</sub> ratio of 0.3 to above 1). NO<sub>x</sub> levels and corresponding ammonia slip levels were recorded during these experiments. As intended, higher urea feeds resulted in lower NO<sub>x</sub> levels. Figure 3 shows the results of these experiment presenting ammonia slip as a function of NO<sub>x</sub> as measured downstream of the SCR (Fig. 3). At exhaust temperature of 350 °C the engine out NO<sub>x</sub> level was approx. 750ppm. At lower NH<sub>3</sub>/NO<sub>x</sub> ratios, meaning NO<sub>x</sub> levels measured downstream of SCR are in the order of 400 ppm and more, all catalysts behave rather similarly, but with the ratio being higher and NO<sub>x</sub> levels lower, the ammonia slip starts to first rise downstream of the V-SCR. With the V-SCR+ASC and Cu-SCR, the ammonia slips form only when NO<sub>x</sub> level is closer to zero (and the corresponding NH<sub>3</sub>/NO<sub>x</sub> ratio 1 and above).

The differences in the performance of the three different SCRs come even more obvious when going down with the exhaust temperature (Fig. 3). In practice, at exhaust temperature of 280 °C, the V-SCR was not capable to achieve any NO<sub>x</sub> reduction (with that high SV in the order of 1000 000 h<sup>-1</sup>). While the Cu-SCR was performing well still at exhaust temperature of 215 °C.

A comparison of ammonia slips with V-SCR and V-SCR+ASC shows what can be achieved with replacing rear part of the SCR by ammonia slip catalyst (ASC). The ASC worked as intended and less ammonia slip was formed while also lower NO<sub>x</sub> levels were achieved with V-SCR+ASC as compared to V-SCR (see upper charts of Fig. 3)

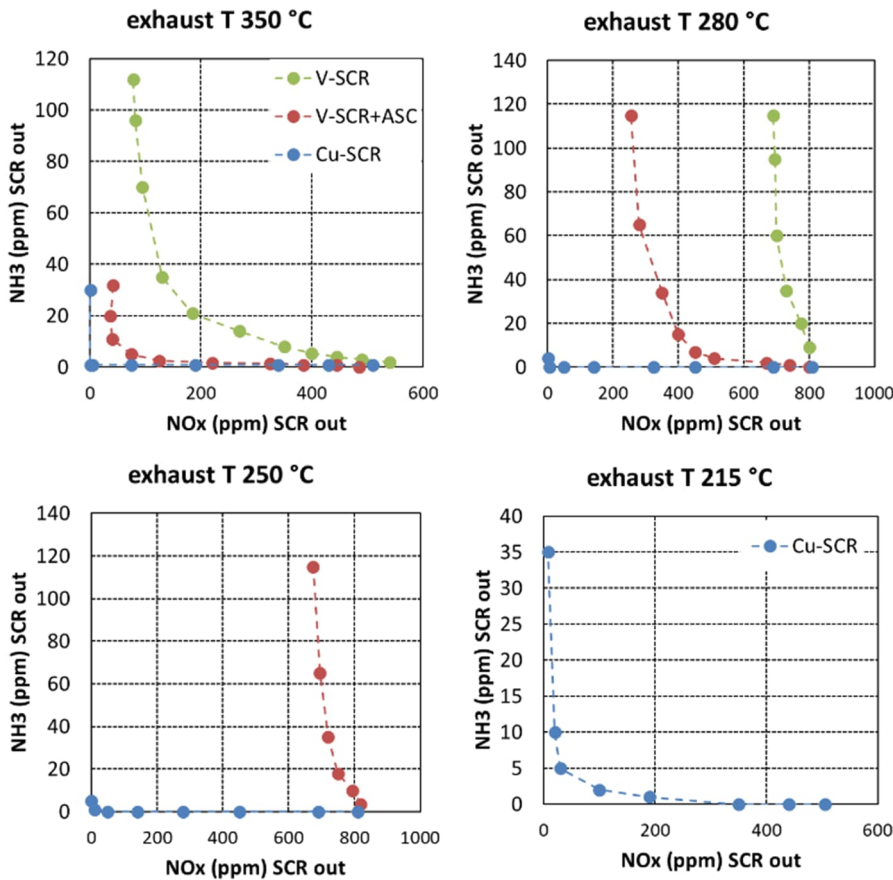


Figure 3 Ammonia slips as a function of NO<sub>x</sub> concentrations measured downstream of the SCR with V-SCR, V-SCR+ASC and Cu-SCR at different exhaust temperatures.

The V-SCR catalysts achieved close to maximum NO<sub>x</sub> reduction at 350 °C. To have a look at this effect of exhaust temperature on the catalyst performance in more detail, NO<sub>x</sub> reduction, ammonia slip as well as N<sub>2</sub>O formation measured downstream of V-SCR+ASC and, also, downstream of the DOC+DPF, are presented at all temperatures in Figure 4. These results are from FTIR measurements conducted simultaneously with two separate FTIR instruments, one placed downstream of the SCR and the other downstream of the DOC+DPF. The NO<sub>x</sub> reduction showed again a decrease when temperature decreases, however this is not that evident when looking at the NO<sub>x</sub> reduction measured downstream of the DOC+DPF that followed the SCR unit. So, it seems that some NO<sub>x</sub> reduction happened still after the SCR unit, over the DOC+DPF. The ammonia slip that was formed at lowest temperature of 250 °C, particularly, has also totally disappeared after the DOC+DPF (middle chart in Fig. 4). NH<sub>3</sub> presence in inlet of DOC+DPF had, however, an undesirable effect on the N<sub>2</sub>O formation, which was found to increase significantly in DOC+DPF (Fig. 4).

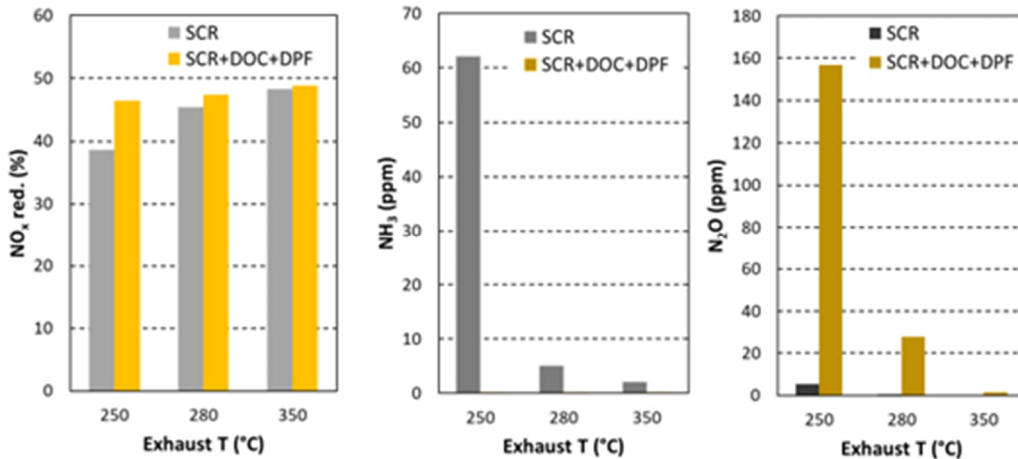


Figure 4 NO<sub>x</sub> conversion together with ammonia and N<sub>2</sub>O concentrations measured downstream of the V-SCR+ASC and downstream of the DOC+DPF with NH<sub>3</sub>/NO<sub>x</sub> ratio of 0.5.

The Cu-SCR catalyst did not show similar dependency on the temperature like the V-SCR+ASC. In Figure 5 the NO<sub>x</sub> reduction, ammonia slip and N<sub>2</sub>O levels are presented for Cu-SCR with NH<sub>3</sub>/NO<sub>x</sub> ratio of 1.05 at 215 °C and 350 °C. Experiments at the lowest exhaust temperature of 215 °C with the urea overdosing using NH<sub>3</sub>/NO<sub>x</sub> of 1.05 showed the only case, when ammonia slip was significantly found downstream of Cu-SCR. Again, at this point, a significant N<sub>2</sub>O formation occurred downstream the DOC+DPF. However, even though the ammonia slip was higher (i.e., near 90 ppm) than in the case of V-SCR+ASC at 250 °C (i.e., near 60 ppm, Fig. 5), the N<sub>2</sub>O formation was lower (i.e., near 40 ppm) with the Cu-SCR at 215 °C than with the V-SCR+ASC at 250 °C (i.e., near 160 ppm, Fig. 5). One reason for this is that the NO<sub>x</sub> (NO & NO<sub>2</sub>) available for the reactions to produce N<sub>2</sub>O is higher in the case of V-SCR+ASC at 250 °C, since that experiment was done with NH<sub>3</sub>/NO<sub>x</sub> ratio of 0.5 – meaning that more than half of the engine out NO<sub>x</sub> is still in the form of NO<sub>x</sub> after SCR as well.

N<sub>2</sub>O formation is based on the surface reaction of N+NO, when particularly platinum (on ASC, DOC and DPF) is efficient in NO dissociation. N<sub>2</sub>O is formed always in NO<sub>x</sub> reduction i.e., by NH<sub>3</sub> or HCs on Pt catalysts. N<sub>2</sub>O can be originated to both NO and NH<sub>3</sub> in these conditions. In addition, N<sub>2</sub>O formation is favored thermodynamically around 200-350 °C [Maunula et al. 2016, Maunula et al. 2020].

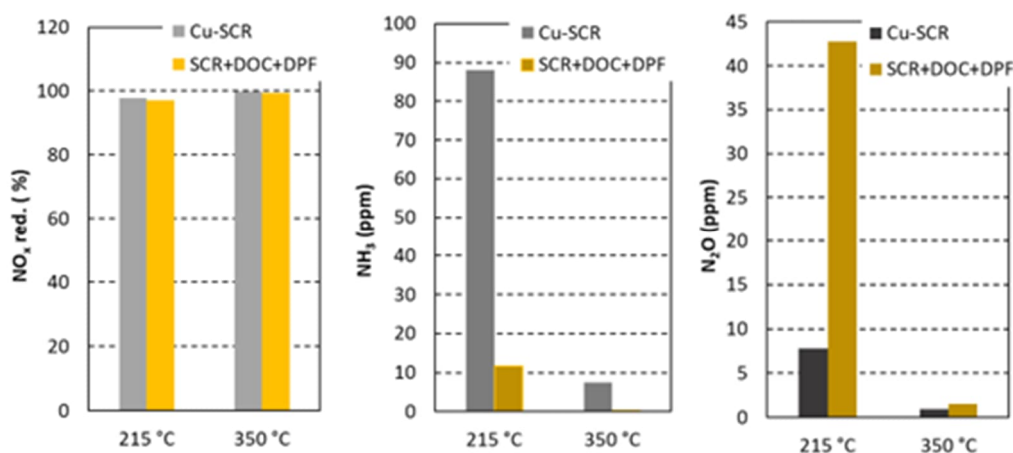


Figure 5 NO<sub>x</sub> conversion together with ammonia and N<sub>2</sub>O concentrations measured downstream of the Cu-SCR and downstream of the DOC+DPF with NH<sub>3</sub>/NO<sub>x</sub> ratio of 1.05.

### 3.3.2 Urea vs ammonia

In addition to utilizing urea water solution as a source of ammonia for SCR reactions, studies were done also with utilizing ammonia gas (from gas bottle) as a reductant. V-SCR+ASC was selected for these studies. The V-SCR+ASC didn't perform too well with urea, making it possible to see whether ammonia utilization might make a difference on the SCR performance. Studies were done with three different exhaust temperatures (250 °C, 280 °C, 330 °C). Similar  $\text{NH}_3/\text{NO}_x$  ratios were utilized with urea water solution and with ammonia gas (Fig. 6). In all cases studied, ammonia gas led to higher  $\text{NO}_x$  reduction than urea solution in the same conditions (same engine out  $\text{NO}_x$  level, exhaust temperature and  $\text{NH}_3/\text{NO}_x$  ratio).

However, the differences in  $\text{NO}_x$  reduction by ammonia instead of urea was not found to be significant in all cases studied and use of ammonia gas instead of urea solution was found to increase the  $\text{NO}_x$  reduction by 2-14%. While the differences of only few percent (approx. 2-5%) are difficult to distinguish from the possible uncertainties involved in the  $\text{NO}_x$  measurement as well as in the urea & ammonia measurement, the higher values are distinguishable. Also, the trend in all the results was clear, in all cases the ammonia utilization led to better SCR efficiency. Based on these results, since utilizing ammonia gas instead of urea water solution is more challenging, ammonia being toxic, the increase in SCR performance seen in present study with the ammonia, might not be high enough to invest in developing new systems for ammonia insertions to replace the urea water solution usage. However, even more benefit from the ammonia usage could be possible at lower exhaust temperatures where urea hydrolysis is not as effective or when utilizing different catalyst chemistry in SCR [Seneque et al. 2016]. And if the SCR sizing is reduced significantly, the volume might not be any more enough for SCR reactions. When the thermal hydrolysis is slow at low temperatures the first part of the SCR volume might be solely utilized for urea hydrolysis [Dae Yim et al. 2004] that is needed before the SCR reactions can have the needed ammonia reactant.

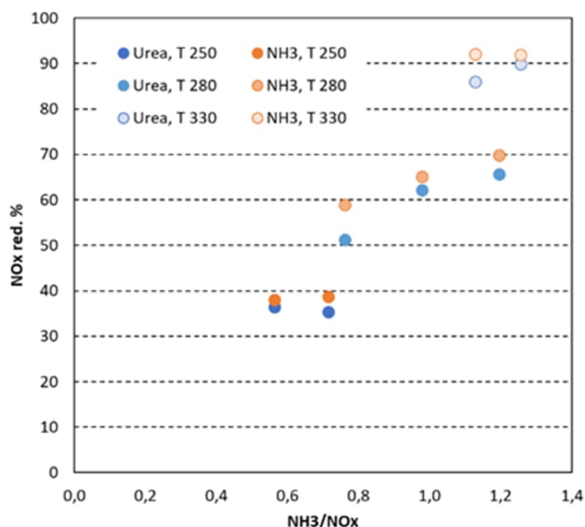


Figure 6  $\text{NO}_x$  reduction as a function of inserted  $\text{NH}_3/\text{NO}_x$  ratio at three different exhaust temperatures utilizing urea and ammonia. Catalyst: V-SCR+ASC.

### 3.3.3 Other emissions

The engine out CO level was measured to be close to 30 ppm. All the SCRs studied had only minor effect on the CO level, while the DOC+DPF was found to remove CO close to zero in all conditions studied. Meaning that the DOC was effectively oxidizing CO in all cases studied. Different hydrocarbon components were analyzed with FTIR, and they all showed low concentrations, in engine out-case the

sum of the analyzed hydrocarbon components was near 13 ppm, and this was effectively decreased already in the SCRs.

The particle emission studies showed that the DPF was effective in decreasing both the PM and PN. The engine out PM level was near  $4 \text{ mg/m}^3$  and when measured downstream of the DPF with all SCRs studied, the level was below  $0,4 \text{ mg/m}^3$  meaning a PM reduction  $>90\%$ . The engine out PN level was  $2-3 \cdot 10^{12} \text{ \#/m}^3$  while the levels downstream of DPF had rather high variation between  $1 \cdot 10^8-1 \cdot 10^{11} \text{ \#/m}^3$ . PM and PN results, obtained from all measurements done downstream of the DPF are presented as a function of exhaust temperature in Fig. 7. We note that no regeneration was forced during the measurements and that the driving history might have an effect on the PM & PN levels measured downstream of the DPF. To study the DPF in detail was not the focus in present study, while the particle measurements were only done to ensure that the DPF is working and decreasing the particle emission level. However, when studying the results, a bit further, there seems to be a trend in both the PM and PN levels measured downstream of the DPF, showing that at higher exhaust temperature, also higher PM and PN levels were recorded. The exact emission level when utilizing different SCRs might have been different, and this might have been due to other things than the SCR itself e.g., the driving history might play a role here. Since this was not studied systematically, we only present the results as a collection of PM & PN recordings, not specifically for one SCR related. Even though, the trend with the particle emission levels increasing with temperature increase, exists. Similar trends have been seen in other studies with diesel catalysts as well. When sulphur is available for reactions, this particle emission increase with temperature increase downstream of a catalyst is explained by sulphate formation [Lehtoranta et al. 2015]. However, similar trend has been observed also in cases where sulphur level is extremely low [Lehtoranta et al. 2017].

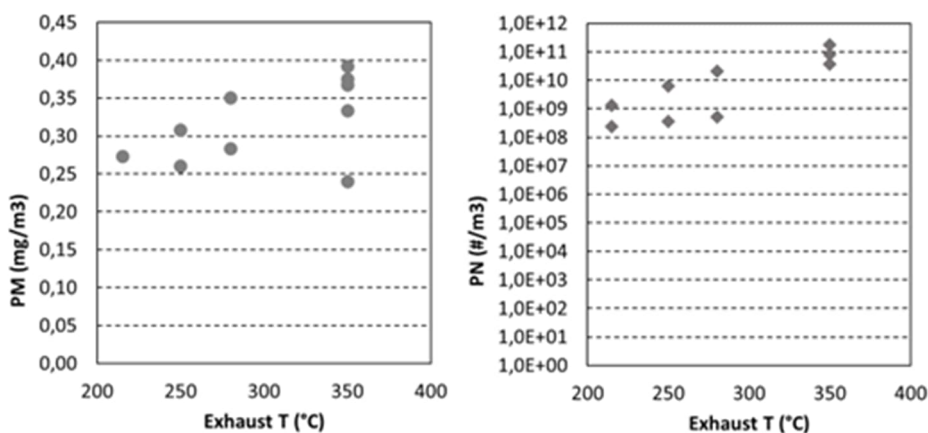


Figure 7 PM and PN as measured downstream of the DPF, as a function of exhaust temperature.

In general, when DPF is combined with DOC, passive regeneration of the DPF is possible by  $\text{NO}_2$  formed from  $\text{NO}$  over the DOC. In this concept, having a SCR upstream the DOC decreased the  $\text{NO}_x$  level and obviously less  $\text{NO}_2$  is then available for regeneration purposes as well. However, the focus with this first SCR unit, a close coupled SCR, is not to achieve the highest  $\text{NO}_x$  reductions at all conditions but to be utilized in conditions where the exhaust temperature is otherwise too low for the  $\text{NO}_x$  reduction downstream of the DPF (i.e., the conventional position for the SCR system). DPF regeneration can be considered to be based mainly on active regeneration methods in the investigated systems where the CC-SCR catalyst is removing a large part of  $\text{NO}_x$  before DOC+DPF (too low  $\text{NO}_2$  concentrations for passive regeneration).

### 3.4 Main findings

The main conclusions from the experiments conducted with a high space velocity (near 100.000 h<sup>-1</sup>) and without NO<sub>2</sub> assistance on close-coupled SCR catalysts in this study are:

- V-SCR was found to perform well only at exhaust temperature of 350°C but not at 280°C or below.
- V-SCR+ASC showed a higher efficiency and achieved higher NO<sub>x</sub> reduction than the V-SCR at similar conditions. As expected, with V-SCR+ASC also less ammonia slip was formed than with V-SCR. ASC is able to enhance itself the low temperature activity of V-SCR catalyst, not only oxidizing ammonia.
- The efficiency of V-SCR+ASC was found to drop significantly at 250°C.
- Cu-SCR was found to perform better than V-SCR even with ASC, particularly at low temperatures, resulting in higher NO<sub>x</sub> reduction together with lower NH<sub>3</sub> slip.
- Cu-SCR was found to be very efficient with a high space velocity at all studied exhaust temperatures from 215 to 350°C.
- Always, when ammonia slip was found downstream of any of the SCRs studied, the following DOC+DPF diminished that ammonia slip. However, in these cases, high N<sub>2</sub>O formation downstream of DOC+DPF occurred as a side reaction. This is obviously not a desired situation, since N<sub>2</sub>O is a strong greenhouse gas. Optimization of the urea feed for SCR mapping is important in controlling the ammonia slip and the formation of N<sub>2</sub>O.
- The DOC+DPF following the SCR unit was found to operate well with all SCR catalysts studied, DPF showing very good particle collection efficiencies and DOC oxidizing any carbon monoxide or hydrocarbons existing downstream of the SCR unit.
- Utilizing ammonia gas instead of urea water solution was found to increase slightly NO<sub>x</sub> reduction, but based on the results of this study, probably not significantly enough. Utilization at lower temperatures (<250°C) might though show better promoting effects.

Based on the results of these experiments with the three types of SCR catalysts, Cu-SCR worked best in the examined conditions. We also note that by modifying e.g., the catalyst sizing and/or the amount of catalyst material one can achieve changes in the catalyst performance as well, so the results from present study correspond to the catalysts of this study. The V-SCR catalyst has a high dependency on NO<sub>2</sub> promotion particularly with these high SVs and a small CC-DOC is planned in future experiments to enhance significantly CC-SCR efficiency. However, further studies are also needed to solve limitations, cover the long-term performance as well as transient operation with CC-SCR catalysts. The second SCR to be placed downstream of the DPF was not included in present study. One of the next steps would also mean including this second SCR in the system and integration of double urea injection to engine and SCR control.

Main results of this task were also published in: SAE Technical paper 2022-01-1016  
 Emission Performance of Closed-Coupled SCR Catalysts To Be Applied for Double-SCR Systems  
 written by Kati Lehtoranta, Hannu Vesala, Päivi Koponen, Teuvo Maunula, Matti Happonen

## 4. Targeting to low PM

---

### 4.1 Target

When starting the CPT project, the target setting was updated with the project partners. Fuel and lubricant compositions are very important to particle filter operation in challenging marine conditions. Especially the ash content is crucial. While the filter collects soot from the exhaust and the collected soot can be cleaned from the filter by regeneration methods, the collected ash removal is not possible in similar way. Therefore, the focus was put on studying this ash accumulation in the DPF. In order to produce ash for the studies a method to generate elevated levels of ash in the exhaust was needed. While the fuel itself contains some ash, the main ash source is the lubricant used in the engines. Obviously, the ash accumulation takes time and for the studies an accelerated way to accumulate ash was needed.

In this task, three different ash generation ways were studied. In the first one a separate ash generator was developed, aiming to have a burner in which a marine fuel doped with significant amounts of high-ash lubricant could be used. Second, the aim was to directly dope the marine fuel going to the engine with the high-ash lubricant (with lower levels than was aimed with the burner system). Third was aiming to inject high-ash lubricant into the intake air of the engine.

### 4.2 Methods

#### 4.2.1 Ash generator

The ash generator was developed both using CPT and VTT's own funding. The ash generator was developed from a commercial boiler and burner. A small power boiler (Jäspi ECO 17 LUX-T) used typically in detached houses was selected as a basis of the system. An oil burner (Oilon BF 1 FUV HC) was selected for the system. The burner was equipped with a small oil nozzle providing oil flow of 1.3 kg/h. The burner is equipped with an internal oil pump. An oil filter and an air removal system were installed in the oil feed line.

The ash generator required auxiliary systems to ensure reliable operation in which the burner is constantly on. A recirculation pump was installed to sustain constant water flow from the boiler to a heat exchanger and back to the boiler. Tap water was used to remove the heat in the exchanger. The flow of cool tap water was controlled with a thermostat, which measured the water temperature in the boiler and adjusted flow of the cooling tap water. The boiler was also equipped with a pressure relief valve and a volume compensator. The boiler has also an electric heater, which can be used to maintain temperature in the boiler and prevent condensation.





Figure 8 Ash generator based on an oil burner and a boiler installed in the eDyna test cell (left). Ash generator in operation (right).

Use of the ash generator in DPF measurements requires a fan and a flow meter, which were installed to supplement the burner system. Schematic of this system is presented in Figure 9. The flow meter was based on an orifice plate and a differential pressure meter. The orifice plate was manufactured in-house and a differential pressure flow meter with voltage output (DPT2500-R8, HK Instruments Oy) was purchased for the system. The output signal from the differential pressure meter can be connected into the eDyna logging system.

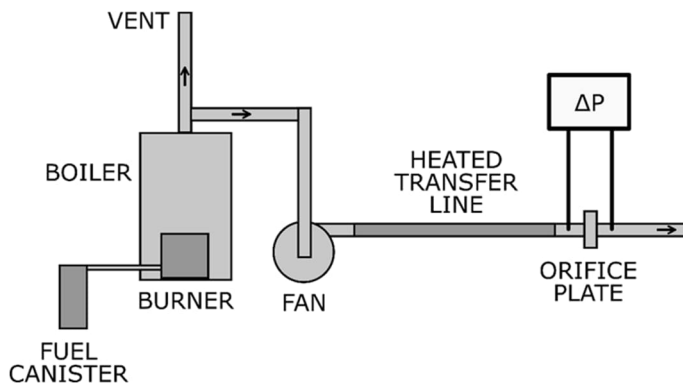


Figure 9 Schematic of the ash generator with additional components used in DPF test measurements.

#### 4.2.2 Doping engine fuel with high ash lubricant

To dope the fuel with lubricant required careful operation. First, the desired lubricant amount was weighed and then it was mixed to the fuel tank with Flux type pump-mixer. After the mixing was ready, the doped fuel was normally delivered to the engine. Different lubricant amounts, resulting to blends containing 0.2% - 2% lubricant, were studied.



Figure 10 Photo of the fuel tank doped with the lube (left hand side) and preparing the lube mix to fuel (right hand side).

#### 4.2.3 High ash lubricant injection to intake air

Another way to introduce the lube addition to the engine combustion was to do that via the intake air. For this method a Gilson Miniplus pump was employed to insert either pure lube or a mix of lube and fuel to the intake air. To control the amount a mass flow meter was used, and the inserted lube canister was also placed on a weigher. Different lubricant injection amounts, between 1-2 ml/min, were studied.

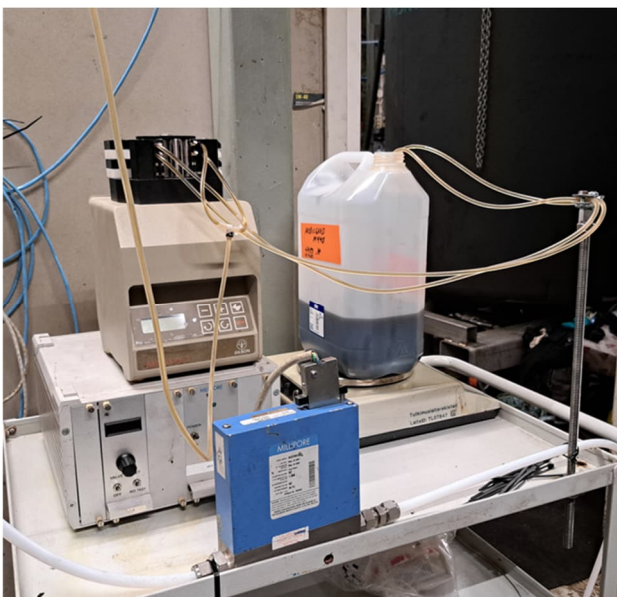


Figure 11 Photo of the setup used to insert lube (or lube and fuel) mix to the intake air.

#### 4.2.4 Test setup and emission measurements

In studying the ash accumulation to DPF with all the above presented three ways to produce ash, the same test bench facility was used (Figure 12). With the VTT's catalyst bench, the exhaust flow through the DPF can be adjusted from 25-120 kg/h and the exhaust temperature range is up to approximately 550 °C.

The test setup was equipped with different measurements devices to study the effect of ash accumulation to DPF operation and regeneration.

Gaseous emissions, including NO<sub>x</sub>, NO<sub>2</sub>, N<sub>2</sub>O, NH<sub>3</sub>, CO<sub>2</sub>, CO and THC, were measured on-line at 20 seconds intervals using the Fourier transformation infrared (FTIR) equipment (Gasmeter DX-4000). Sample for Gasmeter DX-4000 was wet raw exhaust gas at temperature of 180 °C.

Continuous soot measurement was done with AVL Micro Soot Sensor (MSS, photoacoustic method). The results obtained by AVL MSS represent black carbon concentrations in exhaust, and these should be equivalent to the elemental carbon (EC) concentrations measured by thermal-optical analysis (TOA), since OEM calibration of the AVL MSS instrument is based on the TOA.

Continuous PN measurement was measuring non-volatile, solid particle number emissions with DEED+CPC system according to EU Stage V legislation. Before DEED, the sample gas was diluted with eDiluter. Dilution air for eDiluter was dried, filtered and heated.

To measure total particulate matter (PM), The AVL Smart Sampler (SPC) was used for partial flow dilution and sampling of total PM. Partial flow dilution system combined with gravimetric sampling of exhaust particulates is a standardised procedure (ISO 8178). Pallflex TX40 filters were used for PM collections.

Ash accumulated in DPF was determined by weighing the DPF before and after the measurement period. Another method for determining the accumulated ash in the DPF was based on the analysis of ash content of PM and duration of the measurements.

Ash content of PM was determined by using thermal-optical analysis (TOA), which quantitatively analyses the total carbon (TC) content of PM and the rest is assumed to be ash. For the TOA, PM was collected with quartz microfiber Tissuquartz filters pre-cleaned for two hours at 850 °C followed with several days stabilisation. Instrument was Sunset Laboratories Inc's model 4L. In the TOA method, temperature and gas atmosphere is adjusted while continuously measuring the transmission of a laser through the sample matrix. Organic carbon, the original EC, and that produced by the pyrolysis, are oxidized to CO<sub>2</sub>, which is then converted to methane and detected by the FID. Methane is injected into the sample oven providing the calibration of each sample analyzed to a known quantity of carbon. Saccharose is used as an external standard. EUSAAR2 protocol (EN 16909) was used.

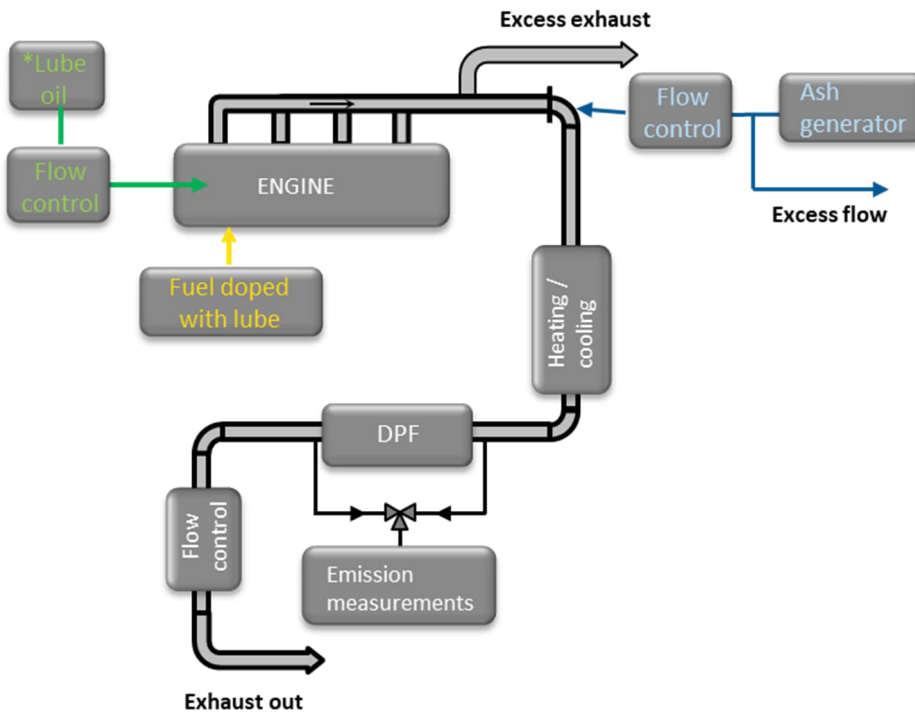


Figure 12 Simplified graphic of the test set-up with all the three ash generation methods (which were used separately).

The DPF elements for the studies were selected together with project partner Wärtsilä and Wärtsilä also provided those samples through their network. Figure 13 below shows a photo of how the element is backed inside a reactor to be studied with the test facility presented above.

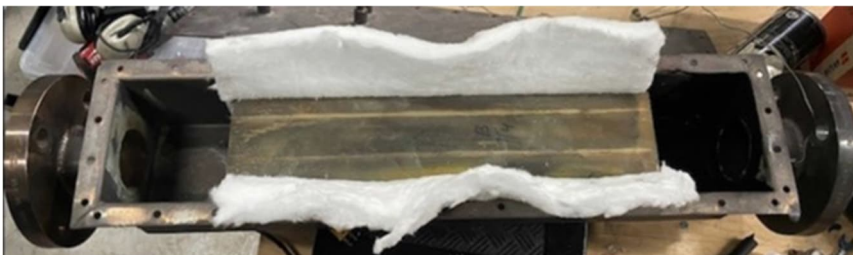


Figure 13 Photo of a DPF element packing inside the reactor.

## 4.3 Results

### 4.3.1 Ash generator study

Almost 160 hours program with a diesel engine, catalyst test bench and a DPF A sample was combined with ash generator. High and low soot modes (HS, LS) were adjusted to accelerated accumulation of soot in certain periods and to accomplish studies of Gas Hourly Space Velocity (GHSV) with engine running on low soot mode. Higher soot concentrations upstream DPF were achieved by decreasing the rail pressure from the OEM settings.

Particulate matter (PM) composition in different test phases is of primary importance for evaluation of the results (Figure 14). Particulate matter in the exhaust from diesel engine contained substantial share of elemental (EC) and organic carbon (OC), and both of these constituents were efficiently reduced by the DPF.

Soot concentrations, commensurable with black carbon (BC) when measured with the AVL MSS instrument, were approximately 18% lower than EC measured by TOA from PM samples (EC). In principle, these should be equivalent, since AVL MSS is calibrated by the EC.

There is no direct methodology for measuring ash concentrations of the exhaust. Indirectly, ash can be derived by subtracting EC and organic carbon (OC) and sulphates from total PM mass. However, a substantial uncertainty is related to this methodology, for example, due to the other constituents that may be present in PM.

Ash content of PM from diesel engine was 1.9 (HS mode) and 0.8 mg/Sm<sup>3</sup> (LS mode), while it was as high as 27 mg/Sm<sup>3</sup>, on average, when ash generator was applied in the test setup. More than ten times higher ash level of the exhaust accelerated ash accumulation in the DPF.

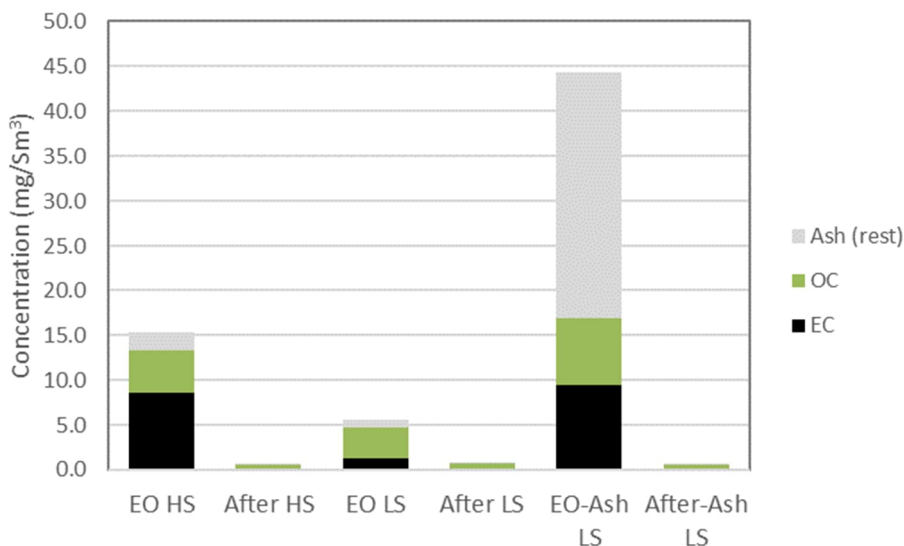


Figure 14. PM composition results, ash generator part. EO = engine out; After = downstream DPF; HS = high soot mode; LS = low soot mode; OC = Organic carbon; EC = Elemental carbon.

Ash accumulation in the DPF over the testing period was 24-38 g based on the weighing of the DPF before and after testing. Calculated ash accumulation was 22 g, respectively. Higher result from weighing than from calculation could be explained for example by accumulation of some heavy organic material in the DPF.

In the ISO 8178 test, soot emission was on average 7.8/0.8 mg/kWh upstream and 0.03/0.003 mg/kWh downstream DPF in the HS and LS modes.

Figure 15 shows NO<sub>x</sub> and total hydrocarbon (THC) concentrations, soot and ash accumulation, regeneration temperature and DPF reduction efficiencies of soot and non-volatile particles. The DPF reduced efficiently soot and particle number concentrations even when ash and soot loading was increased. Pressure difference (dP) over the DPF clearly increased when ash accumulated to DPF, especially at higher GHSV levels.

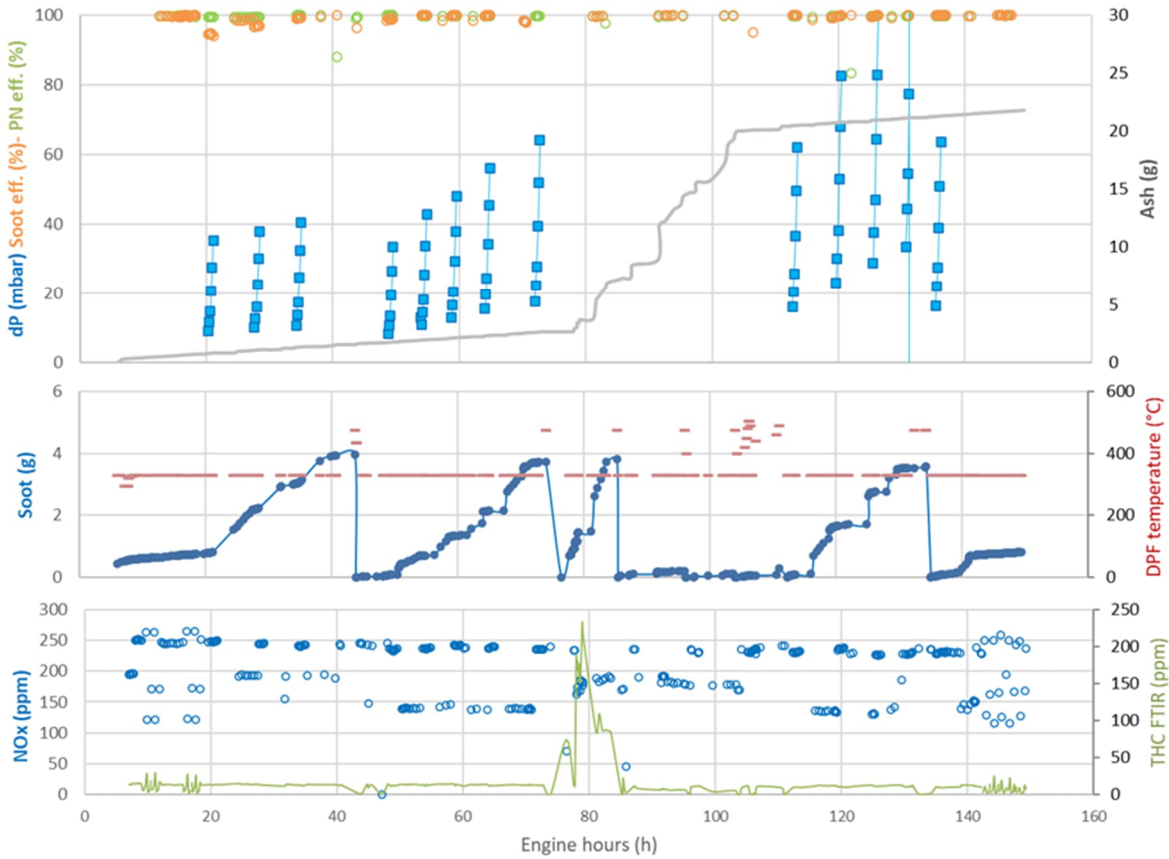


Figure 15. a) Soot and PN reduction efficiencies, ash accumulation and dP at different GHSV levels b) soot accumulation and regeneration temperatures c) NO<sub>x</sub> and THC concentrations over test sequence.

Particle number emissions were reduced efficiently by the DPF in all size classes measured (Figure 16).

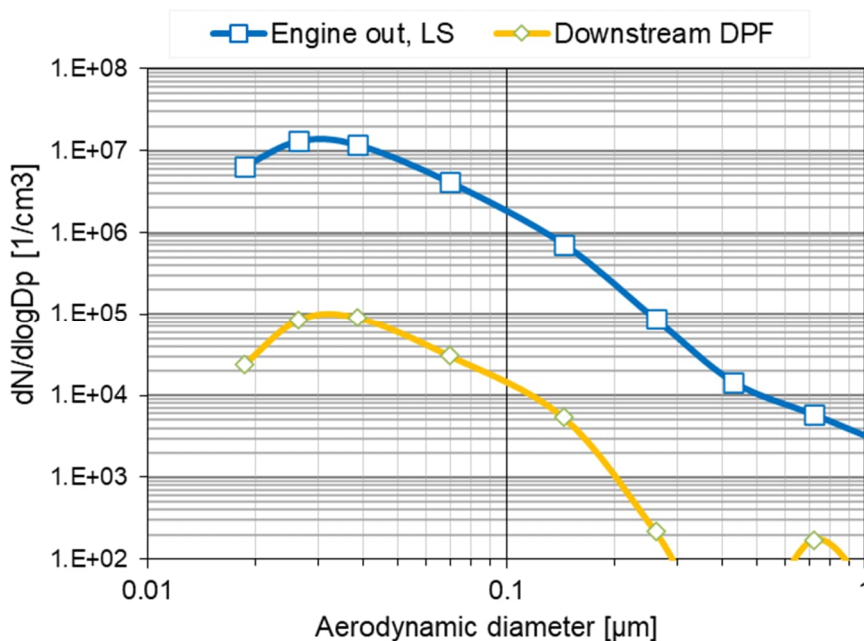


Figure 16. Particle number size distributions upstream and downstream of the DPF, low-soot mode.

### 4.3.2 High ash lubricant injection to intake air

Lubricant injection to intake air was used for the first time in this program. However, expected ash accumulation was not reached, which indicates that a part of lubricant may have not combusted to ash.

Ash concentration analysed was at the level of lower than expected, only  $2 \text{ mg/m}^3$ , and the ash results were in many cases negative (Figure 17). Direct methods for analysing ash from exhaust are not available. In this study, two methodologies, DPF weighing and TOA, were used for ash determination. The difficulties with the ash determination by TOA were not seen in the in the ash generator part, since the high the ash concentrations alleviated the analyses. In this part of work, capability of the TOA methodology used to determine low ash concentrations reliably was revealed. Hence, the ash concentrations analysed are largely estimates. The new procedure was developed to increase reliability of the ash results by using a long sample collection time of 600 seconds. With a long collection time, filters are too dark for determination of the split between EC and OC, while total carbon analysed is quantitative and enables more reliable ash analyses. For the EC/OC analyses, another sample with shorter collection time is needed. Modified PM sampling for TOA was suited better for the ash determination.

Ash accumulated in DPF B1 according to the weighings, 15 g, was in the same order of magnitude as that based on calculations, 19.5 g. In the calculations, assumed ash concentration of  $2.05 \text{ mg/Sm}^3$  was used. Expected ash accumulation would have been as high as 45 g with the lubricant injection to intake air, if complete combustion of lubricant would have realized.

In some cases (A2, B1 benchmark), the TOA results showed higher EC results than the soot concentrations analysed by the AVL MSS, which indicates bias in the EC results and needs to be further investigated. The EC and soot results correlated well in the ash accumulation phase of program. In the PM, share of organic carbon was substantial.

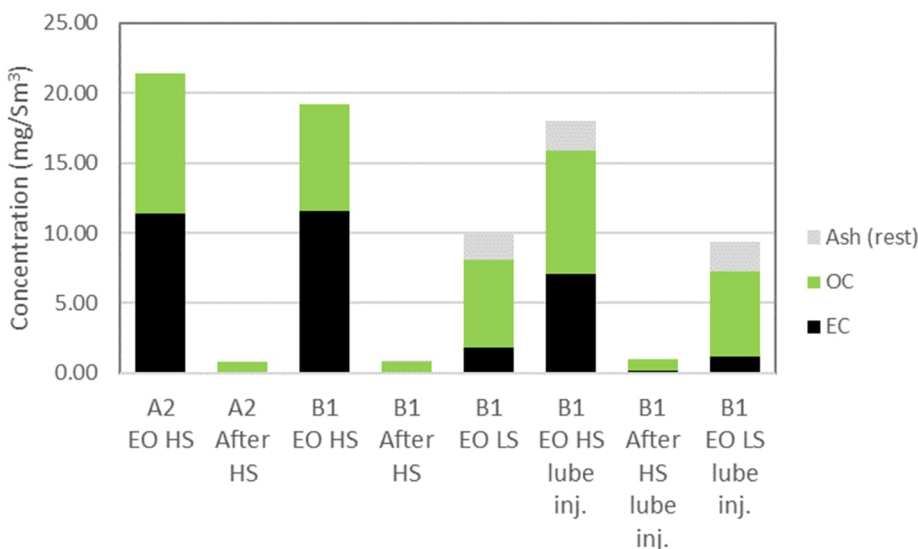


Figure 17. PM composition in the “lubricant to intake air”. EO = upstream DPF; After = downstream DPF; HS = high soot mode; LS = low soot mode; OC = Organic carbon; EC = Elemental carbon.

Before the ash accumulation study, benchmark testing of two DPF samples (A2 and B1) was carried out. Soot was collected in two periods with each DPF, separated by regeneration. At six GHSV settings, back pressures over the DPF B1 were significantly lower than those for the DPF A2 (Figure 18). High reductions of particle number PN23 (non-volatile PN>23 nm) and soot emissions were achieved with both DPFs studied. DPF B1 was selected for the ash accumulation part.

DPF B1 tolerated increased ash levels without substantial effect on the back pressure. Regenerations proceeded well and overall performance of the DPF was good during the ash accumulation part with the DPF B1. Performance of the DPF B1 was also better than that of the DPF A studied earlier. This is assumedly due to the better characteristics of the DPF B1 than the DPF A, however, smooth accumulation of the engine generated ash may also alleviate performance of the DPF when compared to rapid accumulation of ash obtained with burner.

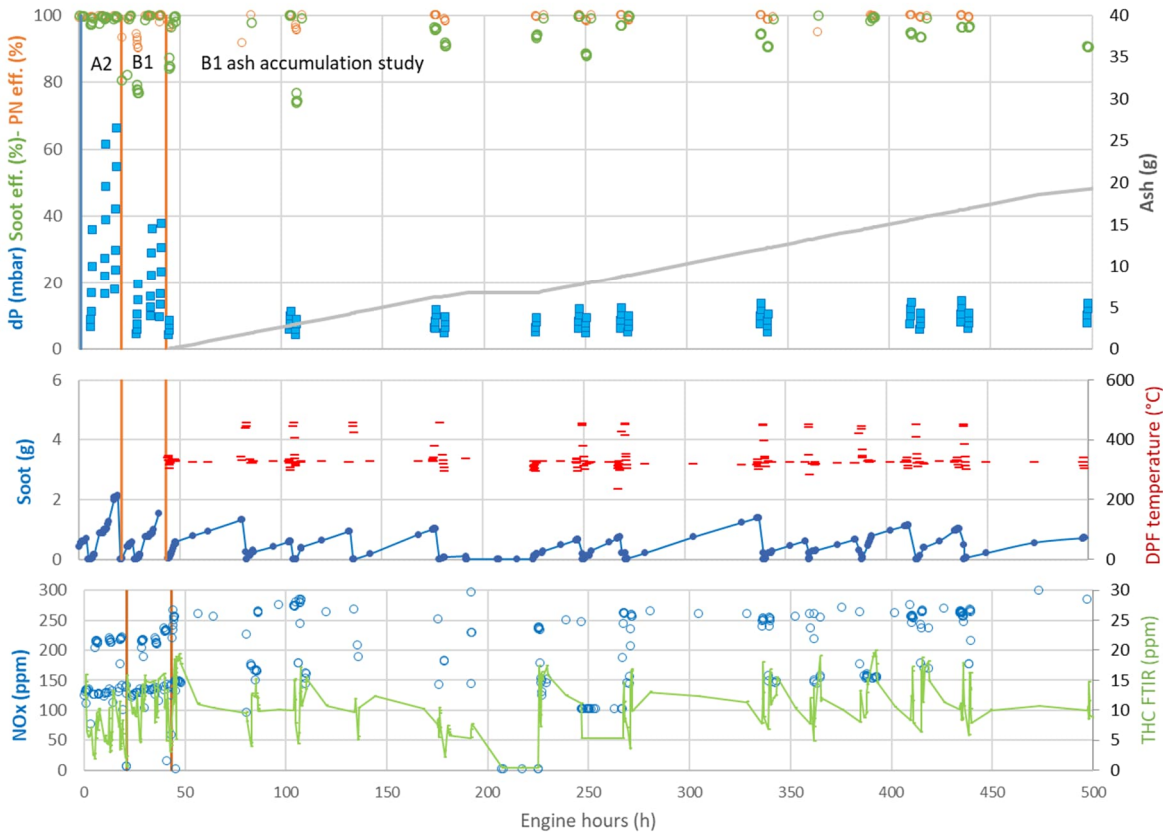


Figure 18. a) Soot and PN reduction efficiencies, ash accumulation and dP at different GHSV levels b) soot accumulation and regeneration temperatures c) NO<sub>x</sub> and THC concentrations over test sequence. In the beginning of test sequence, benchmark testing of DPF A2 and DPF B1 is shown.

Particle number emissions were reduced efficiently by two DPF in all size classes measured (Figure x).



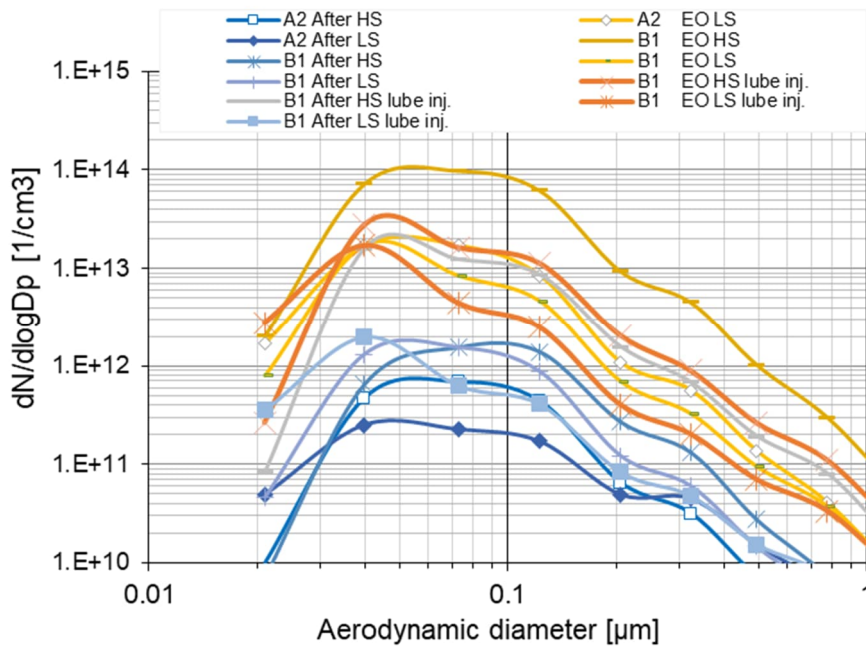


Figure 19. Particle number size distributions upstream and downstream of two DPFs.

#### 4.3.3 Doping engine fuel with high ash lubricant

With DMB fuel doped with high ash lubricants, soot levels of the engine increased to the extent that measurements could not be continued. After changing larger injectors in the engine, a longer time period of engine running was possible, and soot level returned to original level after change to undoped fuel. However, actual DPF study was not carried out with doped fuels within the CPT program.

Comparison of the theoretical ash concentrations obtained with lubricant addition to fuel or intake air is presented in Table 2. Doping fuel with lubricant or adding lubricant in inlet air would theoretically result in many-fold ash accumulation rates compared with the ash level formed naturally from DMB fuel and lubricant. However, these ash concentrations achieved are still modest when compared with those obtained by ash generator.

Table 2. Ash concentrations estimated theoretically with different methods.

	DMB fuel "naturally"	Lubricant "naturally"	Fuel doping A	Fuel doping B	Intake air/ injection
Lubricant	-	Shell Rimula 10W30	MOBILGARD™ M440	MOBILGARD™ M412	MOBILGARD™ M440
Fuel, lub. ash, wt%*	0.0005	0.75	2.5	1.05	2.5
Lubr. in fuel, wt%	-	-	0.2	0.5	-
Fuel, lubr cons.	11.5 kg/h	0.15 g/kWh**	11.5	11.5	
Lubr. cons.	-	-	-	-	1.3 mL/min***
Ash conc. (mg/Sm <sup>3</sup> )	0.1	<0.08	1.4	1.5	4.4

\*Actual ash estimated as half of sulphated ash. \*\*At 40kW, assumption \*\*\*Density 0.915 kg/dm<sup>3</sup>.

## Main findings

Ash generator was designed, built and used in the study. A new system for lubricant injection to intake air was also designed and built for this DPF study.

Improved method for quantification of the ash concentrations in exhaust was developed.

With methodologies used, differences in performances of three DPF samples studied were observed.

Doping fuel with lubricant or adding lubricant in inlet air could result in many-fold ash accumulation rates compared with the ash level formed naturally from DMB fuel and lubricant. Lubricant added in inlet air of a diesel engine did not seem to burn completely.

The highest ash concentrations in exhaust were achieved with in-house designed and built ash generator. However, very high ash generation rate may bias the conclusions on the performance of the DPF, and hence, further validation studies are needed.

- A Scientific publication, Aakko-Saksa et al. in preparation

## 5. Ultralow NO<sub>x</sub> EAT Thermal management

---

### 5.1 Target

High NO<sub>x</sub> reduction efficiency SCR systems need high upstream exhaust gas temperature. In this task, the objective was to investigate the potential of Cylinder deactivation (CDA) technology for NRMM engine exhaust aftertreatment system thermal control. The main focus was in fundamental research, improving the understanding what are the potential opportunities and limitations related to CDA system. This means achievable engine loading, effect on engine efficiency, exhaust gas temperature and emissions. In addition, engine running behaviour was also one objective to be monitored.

### 5.2 Methods

Investigation was done at the VTT engine testing facility on a transient engine dynamometer. The original plan was to perform the research in two phases. During the first phase, the AGCO Power CORE50 engine was mechanically modified for CDA functionality. The goal for the second phase was to acquire commercial variable valve actuation (VVA) system and perform experimental testing with more comprehensive testing conditions. However, in-depth discussions were held with potential VVA system suppliers, but no offer was received that would have led to system acquisition. Therefore, it was decided to perform all testing activities with the mechanically modified test engine.

Mechanical modifications included removal of valve lifters and rocker arms from the deactivated cylinders. This enabled engine operation in CDA mode with cylinders 1&4 and 2&3 active at the time. Figure 20 shows the engine used for CDA testing.

Experimental testing covered following main actions:

1. Reference tests with stock engine setup
2. Reference calibration with VTT ECU (Validation)
3. CDA: Cylinders 1&4 active
  - a. Original parameters

4. CDA: Cylinders 2&3 active
  - a. Original parameters
5. Full engine performance in CDA test points

After reference tests engine control unit (ECU) was changed to VTT own research ECU to allow fuel injection cut-off from the deactivated cylinders. The research ECU was calibrated as close to original parameters as possible, using parameters based on the reference engine, considering the objectives of the project. After calibration actual CDA investigations were started.

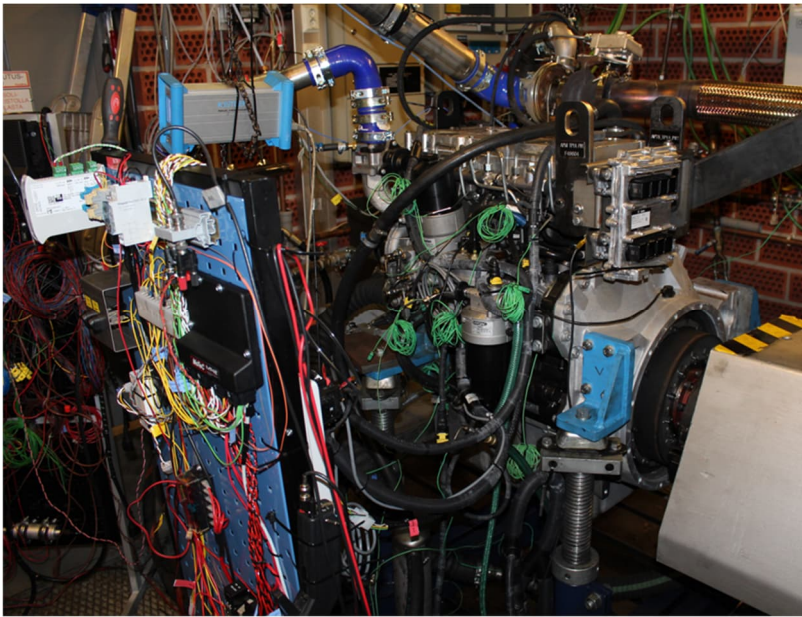


*Figure 20: Test engine used for CDA testing equipped with VTT research ECU.*

### 5.3 Results

The first target in experimental testing was to define operational area that is reasonable for CDA, i.e. engine operates reasonably without crossing the boundary conditions as maximum exhaust gas temperature, abnormal running etc. Figure 21 shows the operation points investigated during the CDA testing. Achievable torque was restricted by the limitation in turbocharging. With only two cylinders active, turbocharger is not working optimally leading to reduced air mass flow and reduced excess air-fuel ratio.

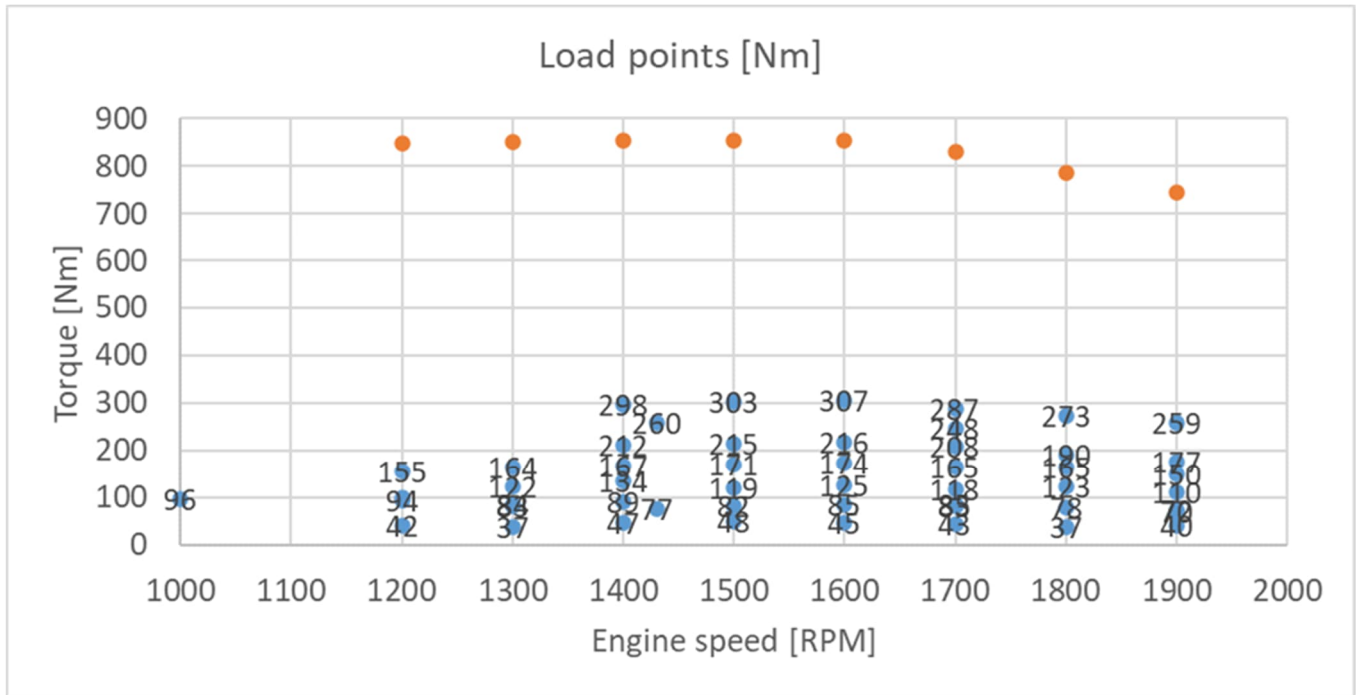


Figure 21: Engine operational area in CDA mode.

In low load area typically diesel engine efficiency is lower than in mid to high loading area. The reason behind this are the less favourable conditions for combustion chemical and physical processes and reduced of gas exchange work. CDA operation allows active cylinders to operate with higher loading, increasing the injection quantity, which improves the combustion chemical and physical processes and thus engine thermal efficiency. Figure 22 shows the relative difference in engine efficiency compared to full engine. It can be seen that CDA mode provides improvements in engine efficiency up to around 150Nm loading area. Above around 150Nm loading, the engine efficiency starts to reduce compared to full engine. With all cylinders activated, the cycle efficiency starts to improve more due to more optimal turbocharging process, i.e. gas exchange process, and improved combustion conditions (chemical and physical processes) which leads to increased engine efficiency. Although, efficiency reduction of about 1 – 2% compared to normally operating engine is not yet significant when high exhaust gas temperature gain is achievable.

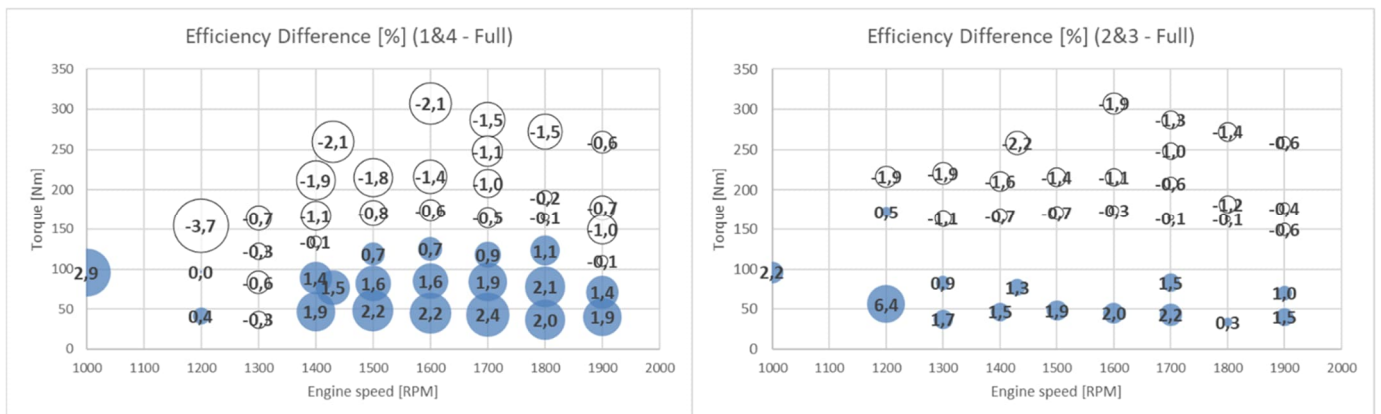


Figure 22: Comparison of engine efficiency in both CDA modes to full engine.

The main motivation for utilization of CDA is in increase of exhaust gas temperature in low loading engine operation area. As emission regulation gets more stringent and the emphasis of in-use operation

conditions increases, the requirement also to secure EAT system operation with high NO<sub>x</sub> reduction efficiency increases. Typically in diesel engines, exhaust gas temperature reduces significantly when engine loading is reduced due to high air to fuel ratio. As a counter measure exhaust gas temperature is increased by reducing air flow through the engine and by using additional, late fuel injections. However, these methodologies have a high penalty in fuel consumption when required temperature increase gets higher. In Figure 23, results of exhaust gas temperature increase compared to full engine can be seen. Results show that there is a high increase in temperature below 200 Nm. Current SCR catalysts temperatures higher than 200°C to achieve above 80% reduction efficiency. In low loading area, below 150Nm, temperature levels are typically well below 200°C. Figure shows that CDA functionality increases temperature over 80°C in 50 Nm range and over 100°C in 100 Nm range. These correspond exhaust gas temperatures between 200°C to 300°C which would allow SRC system to operate with high NO<sub>x</sub> reduction efficiency.

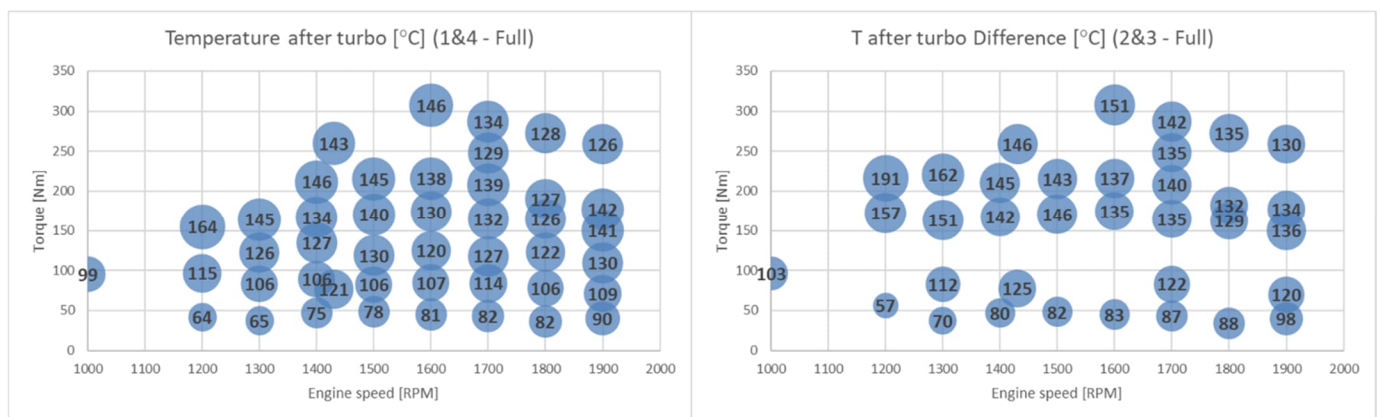


Figure 23: Exhaust gas temperature difference compared to full engine.

As described related to engine efficiency, higher injection quantities tend to increase brake thermal efficiency due to improved combustion. In addition, typically diesel engines have a fixed trade-off between fuel consumption and NO<sub>x</sub> emissions with the given engine components, i.e. keeping the engine combustion related components constant reduction in fuel consumption leads to increase in NO<sub>x</sub> emissions and vice versa.

Figure 24 shows the CDA mode results which suggests mostly lower NO<sub>x</sub> emissions compared to full engine operation. Especially in the engine operation area with most interest, i.e. below 150 Nm, the NO<sub>x</sub> emissions were lower even up to 20%. This would suggest that the fuel consumption versus NO<sub>x</sub> emissions trade-off is different in CDA mode. However, the reason for reduced NO<sub>x</sub> emissions is based on reduced air-fuel ratio during the combustions. Reduced excess oxygen content reduces the formation of thermal NO<sub>x</sub> during the combustion even though higher fuel injection amount increases the penetration of fuel jet and released energy. In addition, reduced air mass flow also reduces also exhaust mass flow which have an effect on mass-based emissions.

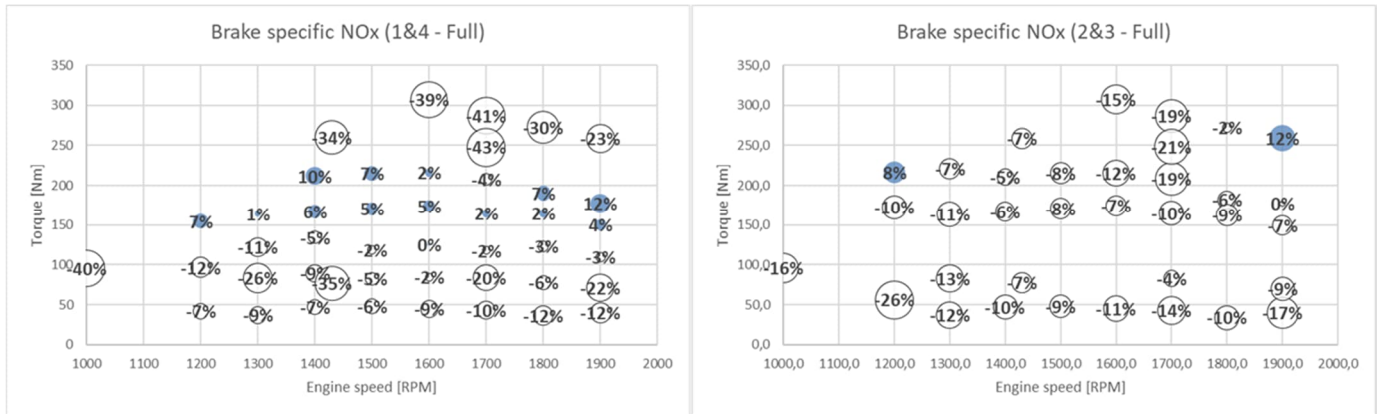


Figure 24: Difference in brake specific NO<sub>x</sub> emissions compared with full engine results.

Surprisingly, PM emissions showed high reduction, even close to 60%, in most of the engine operation points as can be seen in Figure 25. Only high engine speed with low loading showed increase in PM emissions. The reason for the high reduction in mass-based PM emissions is two folded. Higher cylinder loading leads to higher injection pressures and better fuel-air mixture formation which increases the oxygen content in the combustion zone. In addition, increased temperature during the combustion due to higher injection quantity also improves oxidation of particulate matter during the late combustion phase in the burned gases zone. On the other hand, reduced air mass flow means also reduced exhaust gas mass flow, which can be seen in lambda values in Figure 26. As PM emissions are originally measured in mg per cubic meter, leads the reduced mass flow also reduced volume flow and eventually reduced PM emissions in mass bases. Interestingly, high engine speed and low engine loading yielded high PM emissions. There is clear increasing trend seen in the Figure 25 for PM emissions in this region. As a counter measure, PM emission in this region could be most probably greatly reduced by recalibrating the engine control unit for higher injection pressure which, as described above, reduces soot formation.

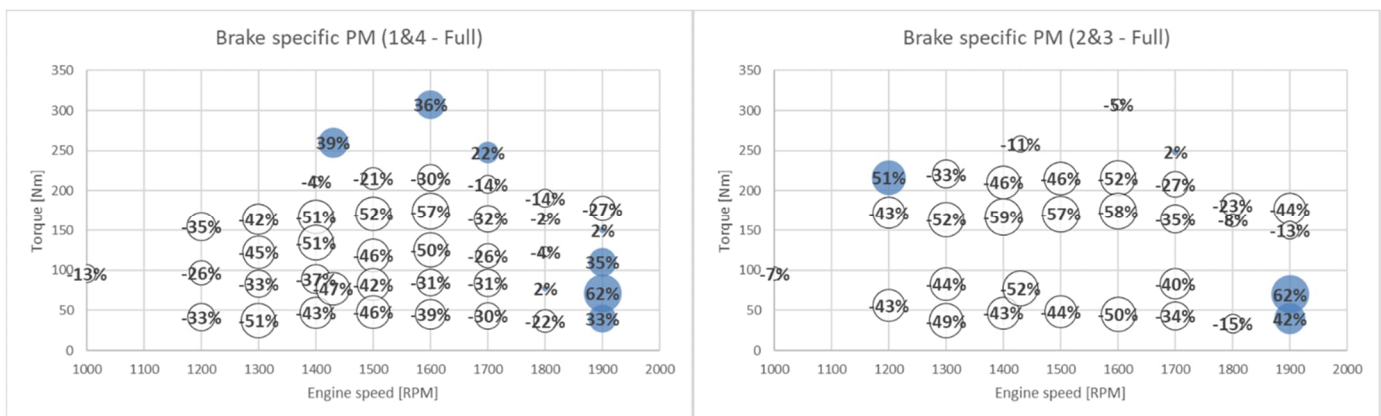


Figure 25: Difference in brake specific PM emissions compared with full engine results.

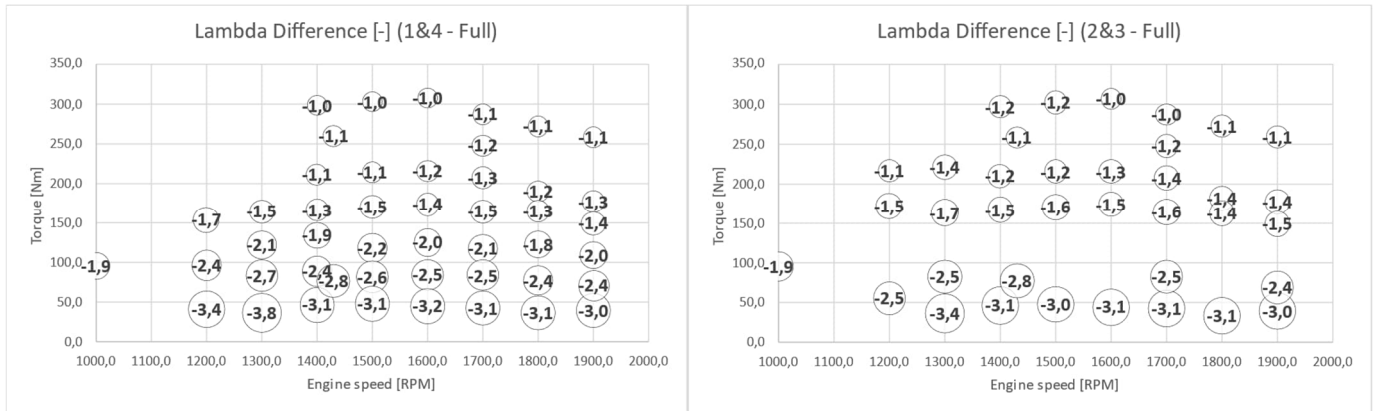


Figure 26: Difference in air to fuel ratio compared to full engine.

## 5.4 Main findings

As a conclusion, CDA technology as such is a great technology for EAT thermal management. It provides high potential in increasing the exhaust gas temperature without compromising the engine efficiency and emissions. However, the potential is highly restricted in the lower engine loading area. For the engine used in the research, the threshold loading without remarkable loss in engine efficiency (less than 2%) was around 200 Nm.

Main take-aways:

- CDA mode can provide roughly 210 °C post turbo temperatures starting from 50 Nm loading range. This means increase in temperature between 60-140 °C depending on the engine load and speed.
- BSFC (brake specific fuel consumption) was 5-10% higher in CDA mode up to 100 Nm of torque and around 150 Nm on par with full engine. Above 150 Nm area BSFC starts to increase compared to full engine operation.
- NO<sub>x</sub> emissions were comparable, or slightly lower as with full engine.
- PM emissions were lower under 200 Nm load range compared to full engine operation. PM emissions were highest on rated speed and low loading range they were higher than with full engine. Up to 150 Nm of torque, PM emissions were 20-50% lower compared to full engine. PM emission could be reduced with recalibrating the ECU for higher injection pressures in the mentioned areas.

## 6. Towards Hydrogen-fuelled engine demonstrator

### 6.1 Target

Hydrogen as a fuel provides interesting carbon free renewable energy option for NRMM. As a carbon free fuel, its combustion with air produces only water and NO<sub>x</sub> emissions. Hydrogen provides also many interesting chemical properties for combustion like wide ignition range and high flame propagation speed which are beneficial for combustion efficiency. However, it has also properties that are challenging for internal combustion engine combustion like low ignition energy and short flame quenching distance. Low ignition energy may lead to unintended start of combustion (preignition) and short flame quenching distance to combustion of oil on the liner surface.

The target of the hydrogen ICE research at VTT was to build in a cooperation with AGCO Power a new spark-ignited test engine that utilizes hydrogen as a fuel. Engine was be equipped with hydrogen direct injection and specially designed combustion related components such as piston bowl, compression ratio, intake manifold and ports designed in the AGCO Power company project.

Objectives for testing were:

- Obtain first experiences of hydrogen combustion and its potentiality.
- Perform measurements on EU Stage V Non-Road Steady Cycle (NRSC) and other steady test points and compare results against Stage V legislation.
- Study the performance and boundaries of hydrogen fuelled engine.
- Formulate understanding and deepen the knowledge of the special characteristics that hydrogen requires from internal combustion engine in construction and control wise.
- Formulate an understanding of possibly required exhaust gas aftertreatment system.

VTT's high-speed engine test facility will be used for the test program. Test facility will be equipped with the special safety instruments required for hydrogen.

## 6.2 Methods

Research work was done at the VTT facilities in Otaniemi Espoo. Research included test setup preparation and experimental engine research. VTT work was divided in two parts:

1. Preparation of the hydrogen test setup
2. Research activities with H<sub>2</sub> direct-injected spark-ignition engine

Preparation of hydrogen compliant engine test cell was done in parallel with the VTT internal infrastructure project, which focused on general hydrogen infrastructure preparation. Figure 27 shows the hydrogen storage at the outside of the test facility. Hydrogen is fed into the facility from the storage and then separately into different test cells. Figure 28 shows test automation instrumentations used for controlling the Nitrogen and Hydrogen feed into the engine. Nitrogen is used for flushing the engine after the hydrogen feed is shut down and to reduce oxygen content in the crankcase.

Test cell preparations included planning and implementation of test automation, piping, valves and other instrumentation required for safe operation with Hydrogen. Preparation activities were mainly done during 2022 before the actual testing activities.





Figure 27: VTT Hydrogen storage at the outside of the test facility.



Figure 28: Test automation components for controlling the Nitrogen and Hydrogen feed into the engine.

Test engine was based on the AGCO Power new CORE50 engine. Figure 29 shows the engine and its installation on engine dynamometer. Engine was equipped with direct-injection fuel system designed for spark-ignition combustion. Also, the engine control software was specially designed for Hydrogen combustion with lean combustion strategy.

Figure 30 shows the schedule and activities conducted during the research. Main blocks and actions done during the research are listed below:

- Engine research during first half of 2023 (February – June)
  - Engine first firing
    - H<sub>2</sub>-infrastructure functionality
    - Engine basic functionality
    - Dyno and ECU control interfaces
    - Data logging and control

- Basic calibration of actuators
- Ignition and injectors basic functionality
- Engine calibration and combustion research
  - Torque build-up
  - Basic combustion fundamentals (knocking, temperature levels, lambda control etc.)
  - Combustion research (start of injection, start of ignition, injection pressure, lambda etc.)

Testing was done in representative engine load points. It was decided during the project that at this point there is no need for conducting actual emission test cycles as ISO-8178 or other. The focus was set on the investigation of the basic phenomena and potential of hydrogen combustion.

Boundary conditions for engine exhaust back pressure, intake pressure, charge air cooler pressure drop and charge air temperature were set to representative values.

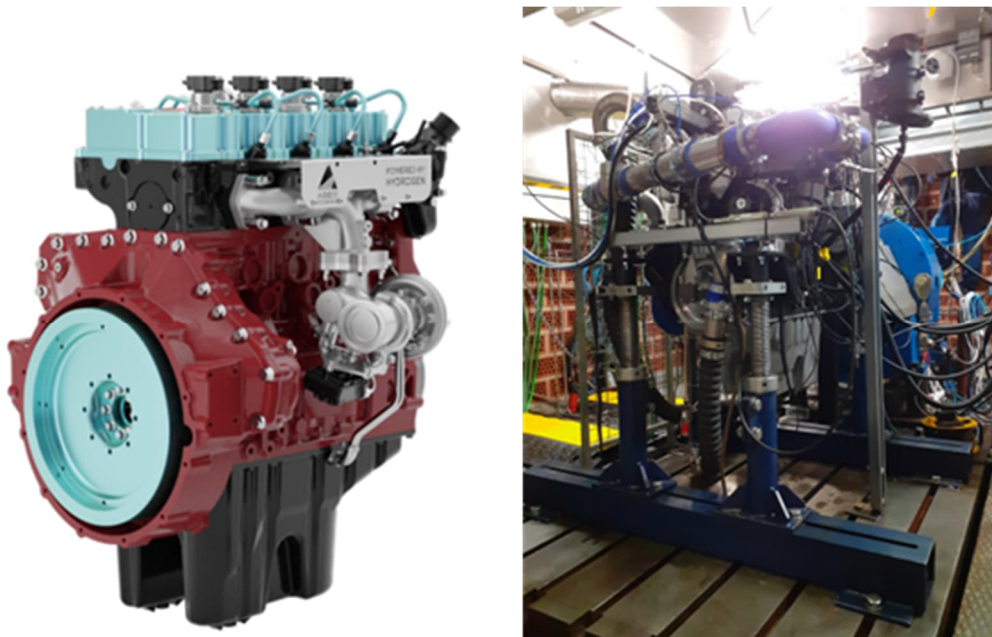


Figure 29: Figure of the engine used for testing.

Activity/Month	January	February	March	April	May	June
Engine installation & Lab functionality checks						
Engine first firing tests and basic functionalities calibration						
Torque build-up testing						
Combustion research (Effect of lambda, railP, start of injection, start of ignition)						

Figure 30: Schedule for the testing.

## 6.3 Results

Hydrogen combustion research included an extensive engine base calibration to achieve sufficient state with engine control system. This was necessary action for ensuring correct functioning of the engine control unit.

Engine performance was tested with a few operation points. In this report, results are shown and discussed only based on two test points as they were fundamentally similar also in all other test points. Figure 31 shows the test points and red circle on it illustrates the reference test point (1600 rpm and 9 bar BMEP) on which all following results are compared. Obtained engine efficiency and NO<sub>x</sub> emission results on the reference point were set 100%.

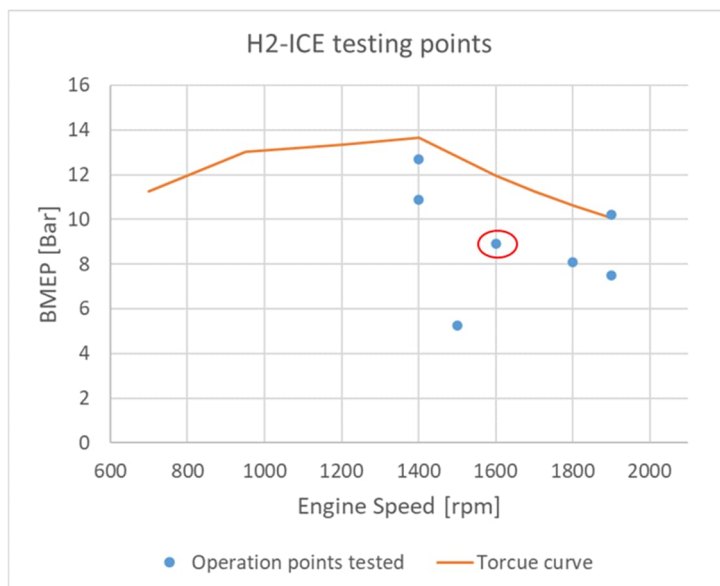


Figure 31: Operation points tested and a reference test point on which results are compared.

Hydrogen lean combustion in SI-engine differs in many ways from traditional diesel combustion in NRMM engines. Hydrogens low ignition energy and high flame speed allows use of high air-to-fuel ratio which is beneficial for gas exchange work and thus on engine efficiency. Figure 32 shows the effect of lambda and injection timing on the engine efficiency. Results in figure clearly indicates that the overall engine efficiency remains rather constant in wide lambda window. By increasing the lambda from 1.85 to 2.35, the efficiency remains within  $\pm 1\%$  of the reference value (circled in red). Efficiency starts to drop rapidly when the lambda value is increased further above 2.5. Also, the difference in start of injection between  $131^\circ$  and  $140^\circ$  BTDC (before top dead centre) seems not have effect on the efficiency. This indicates that there is not big difference in mixture formation that would impact combustion efficiency, i.e. difference in local air-fuel ratio is not significant enough on combustion efficiency wise. Figure 33 shows relative cylinder pressure and heat release at 1500 rpm and 5.25 bar BMEP for three different lambda levels. Using the same reference point as in Figure 32, the change in efficiency is from 89% to 88% and to 78% of the reference efficiency with increasing lambda. It explains how the excess air ratio affects the engine efficiency. The increasing lambda value slows down the heat release, thus prolonging the combustion duration. By increasing the lambda from 2.3 to 2.8 it has only a minor effect on the engine efficiency. Reduced heat release rate is compensated by the improvements in gas exchange work and reduced heat losses. By increasing the lambda even further to 3.2 the engine efficiency is greatly reduced. Gains in gas exchange work does not compensate the implications of the low heat release rate on combustion efficiency.

Engine knocking was limiting the lambda value in tested operation points. Practically lambda value of 1.85 or 2 was the lowest possible without knocking phenomena. This has a huge effect on attainable

loading in the low engine speed and high load region where availability of excess air is restricted by the turbocharger capability to provide boost pressure.

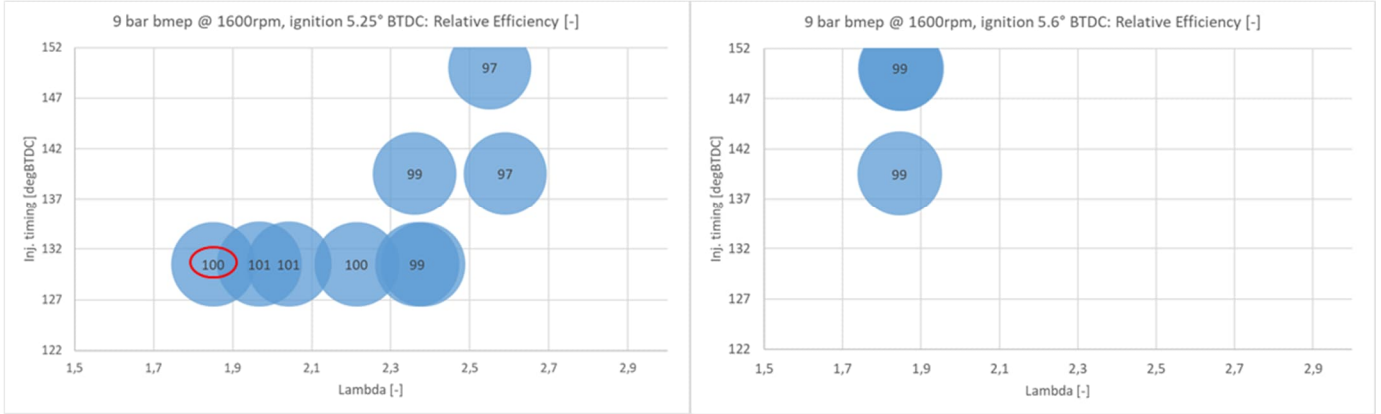


Figure 32: Relative efficiency at 1600 rpm and 9 bar BMEP as a function of lambda and injection timing with ignition angle 5.25° (left figure) and 5.6° (right figure) BTDC.

Averaged (CYL1-CYL4) results for different lambda values

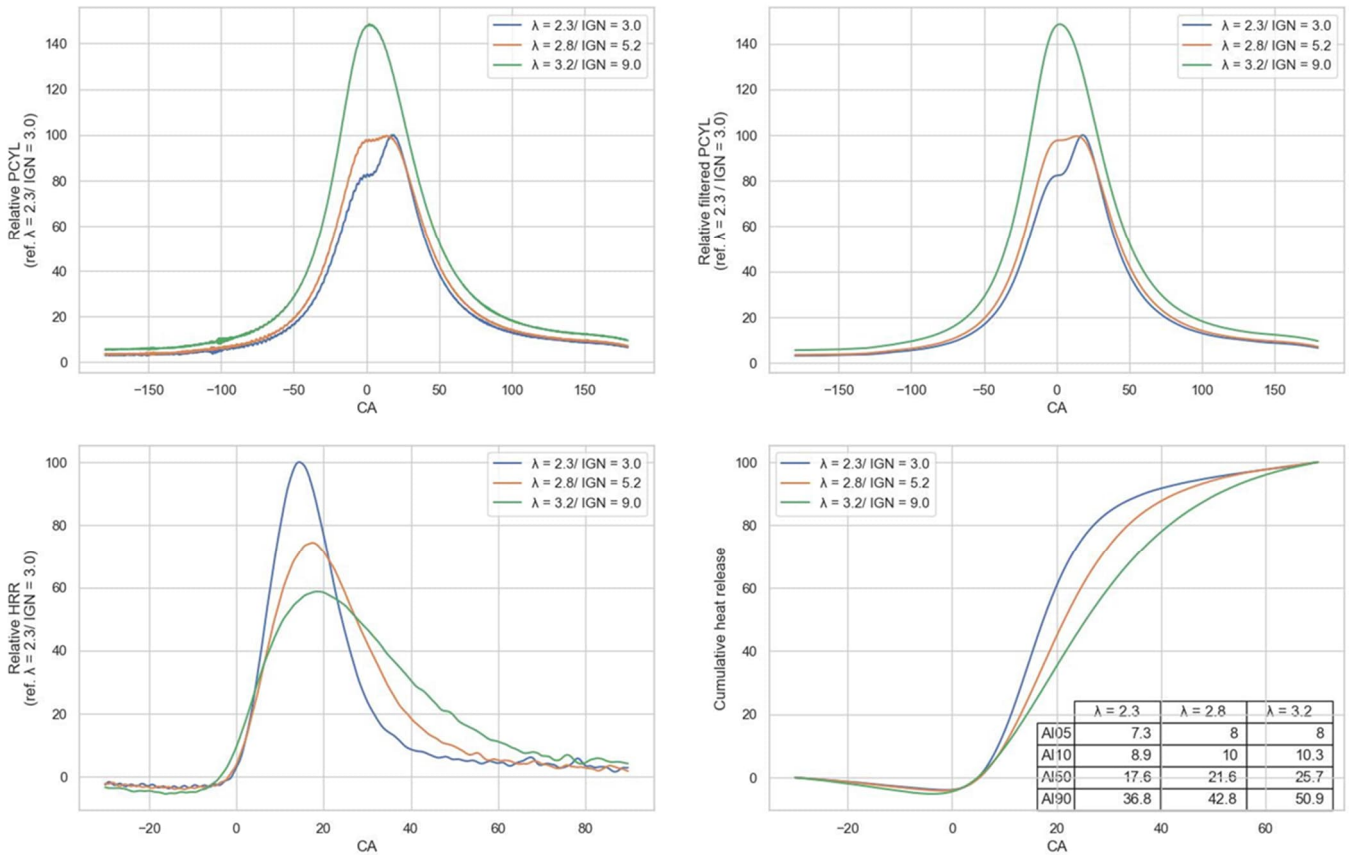


Figure 33: Relative cylinder pressure and heat release as a function of lambda at 1500 rpm and 5.25 bar BMEP.

The hydrogen spark-ignited combustion seems to be rather tolerant in regard to engine efficiency even for rather big changes in lambda. However, the situation is not the same for NO<sub>x</sub> emissions. Figure 34

shows relative  $\text{NO}_x$  emissions as a function of lambda and injection timing similarly as Figure 32 shows efficiency. It clearly shows how big effect lambda has on  $\text{NO}_x$  emissions. By increasing the lambda from the 1.85 to 2.35,  $\text{NO}_x$  emissions are reduced to 8% of the reference value with 1.85 lambda. In addition, injection timing has also an effect on  $\text{NO}_x$  emissions. With around  $10^\circ$  crank angle earlier time of injection  $\text{NO}_x$  emissions can be reduced with around 10% points. Clearly the effect of injection timing on  $\text{NO}_x$  emissions is not as significant as with lambda.  $\text{NO}_x$  formation (mainly thermal  $\text{NO}_x$ ) is highly relative to temperature inside the cylinder. Thus, the significant effect of lambda (excess air ratio) on  $\text{NO}_x$  emissions formation is explained by the lower local temperature in and around the flame front due to higher amount of fuel released energy shifted into internal energy of gases in the cylinder (air and burned mixture gases).

Regarding the exhaust gas reduction technology there might be at least two feasible options. Engine control unit is possible to be calibrated so that the  $\text{NO}_x$  emissions below or close to the current Stage V emission regulatory limit values are possible to achieve. Options then are lean  $\text{NO}_x$  trap or SCR system. Lean  $\text{NO}_x$  trap would require that in static and less transient engine operation points  $\text{NO}_x$  emissions are calibrated below the regulatory limit value. In engine operation situations where lambda value momentarily drops significantly, high  $\text{NO}_x$  emissions need to be handled with lean  $\text{NO}_x$  trap. In case of SCR system, engine out  $\text{NO}_x$  emissions could be calibrated so that optimum between the catalyst cost and  $\text{NO}_x$  reduction performance is met. As such SCR system can reduce  $\text{NO}_x$  emissions even up to 99% from the engine out level.

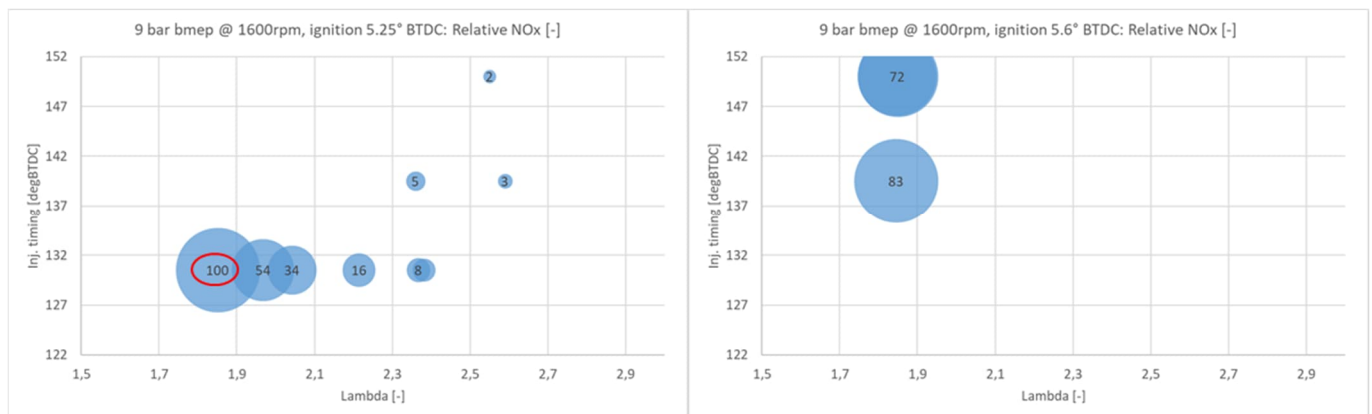


Figure 34: Relative  $\text{NO}_x$  emissions at 1600 rpm and 9 bar BMEP as a function of lambda and injection timing with ignition angle  $5.25^\circ$  (left figure) and  $5.6^\circ$  (right figure) BTDC.

Figure 35 shows the effect of lambda on exhaust gas temperature. With higher lambda value there is more air mass inside the cylinder to be heated which reduces the exhaust gas temperature. By increasing lambda from 1.85 to 2.35 reduces exhaust gas temperature by around  $70^\circ\text{C}$ ,  $440^\circ\text{C}$  to around  $370^\circ\text{C}$ . Time of injection seems not have effect on exhaust gas temperature. This is explained by the similar behaviour with the engine efficiency.

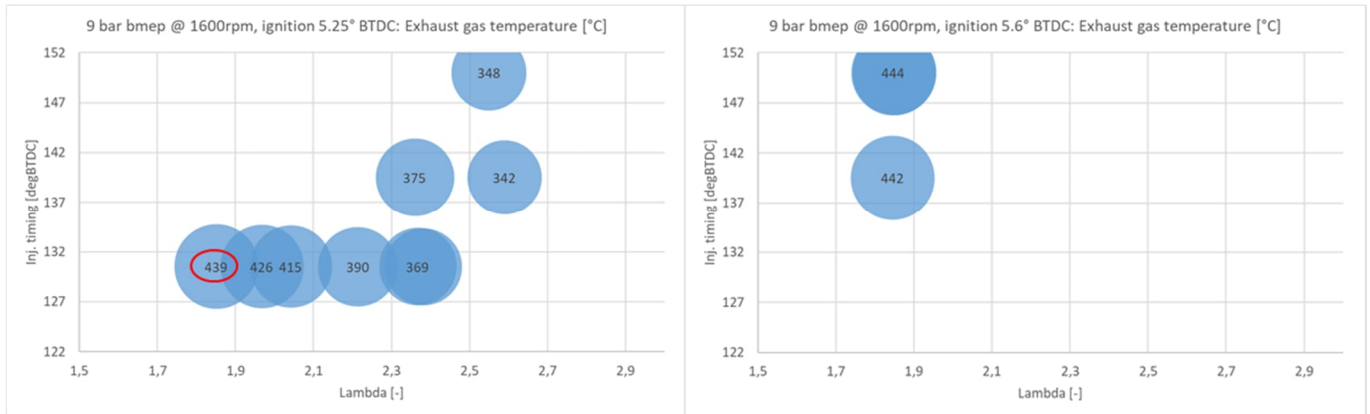


Figure 35: Exhaust gas temperature at 1600 rpm and 9 bar BMEP as a function of lambda and injection timing with ignition angle 5.25° (left figure) and 5.6° (right figure) BTDC.

In general, Hydrogen using lean, spark-ignited combustion allows nice opportunities for engine calibration. High efficiency is attainable with wide lambda window. This allows simultaneously high engine efficiency and low NO<sub>x</sub> emissions. This is something that is not witnessed in typical diesel combustion where there is clear trade-off between the engine efficiency and NO<sub>x</sub> emissions. Figure 36 highlights this effect by showing the change in efficiency and NO<sub>x</sub> emissions in few operation points (green circles) as a function of lambda. Here the NO<sub>x</sub> emissions and efficiency are compared against the reference point at 1600rpm and 9 bar BMEP (Figure 32). The shown figures illustrate the range of NO<sub>x</sub> emissions and efficiency for lowest and highest lambda within each operation point. For example, at 1400rpm and 11bar BMEP with highest lambda the NO<sub>x</sub> emissions are only 3% of the NO<sub>x</sub> emissions in the reference point while maintaining similar engine efficiency (96% of the reference efficiency). On the other hand, with lowest lambda in the same point the engine efficiency is slightly better than in the reference point, but NO<sub>x</sub> emissions are increased significantly (160%).

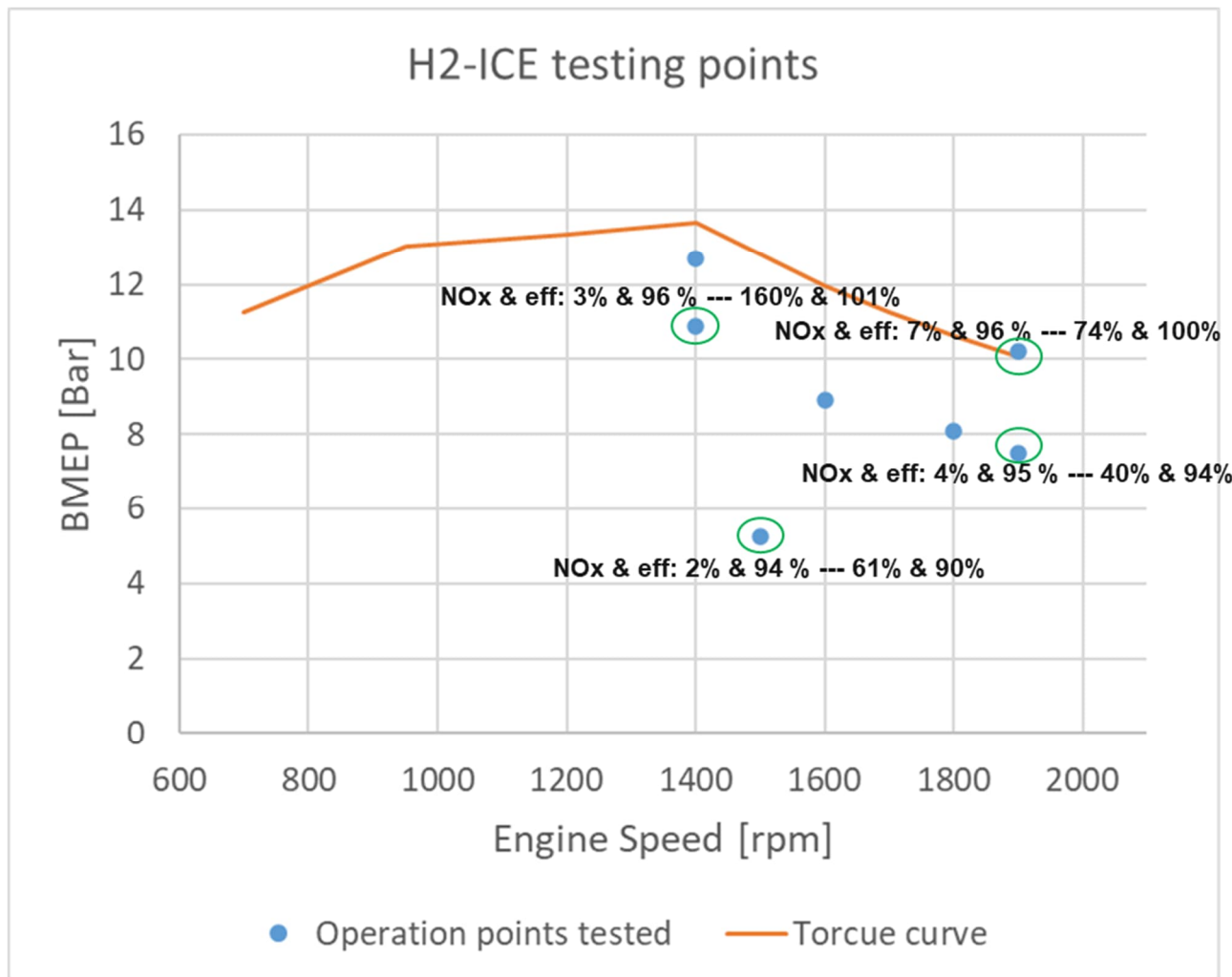


Figure 36: Overview of H<sub>2</sub> engine NO<sub>x</sub> emissions correlation with the efficiency. Reference point 1600 rpm and 9 bar BMEP.

## 6.4 Main findings

Hydrogen lean combustion in spark ignited NRMM engine provides extremely interesting measure for zero carbon emissions. It is capable of close to diesel-like efficiency with low engine-out NO<sub>x</sub> emissions and with no soot or hydrocarbon or carbon monoxide emissions. Below is highlighted the main findings in this project:

- High efficiency, close to diesel, is possible on wide operational area (RPM & torque)
- Low NO<sub>x</sub> emissions possible on wide operational area (RPM & torque)
- High efficiency and low NO<sub>x</sub> emissions possible to meet simultaneously with multiple parameter combinations
  - In some operation points, even the highest efficiency resulted close to the lowest NO<sub>x</sub> emissions
- Torque build-up on low-end torque area is limited due to lack of air i.e. challenge for turbocharging
- Sensitivity to excess air ratio (lambda)
  - Limitations to torque

- Positive effect on post-turbo exhaust gas temperature, typically between 300 °C – 400 °C
- However, operational window is limited by the knocking tendency – This is closely linked to lambda
  - Pre-ignition caused by hot surface or other mechanism leading to ignition of hydrogen
  - Traditional knocking caused by autoignition outside the flame front

## References

---

Dae Yim, S., Jean Kim, S., Hyun Baik, J., Nam, I., Sun Mok, Y., Lee, J.-H., K. Cho, B., and H. Oh, S., "Decomposition of Urea into NH<sub>3</sub> for the SCR Process," *Industrial & Engineering Chemistry Research* 43(16):4856–4863, 2004, doi:10.1021/ie034052j.

Harris, T.M., Mc Pherson, K., Rezaei, R., Kovacs, D., Rauch, H., and Huang, Y., "Modeling of close-coupled SCR concepts to meet future cold start requirements for heavy-duty engines," *SAE Technical Papers* 2019-April(April), 2019, doi:10.4271/2019-01-0984.

Kasab, J.J., Hadl, K., Raser, B., Sacher, T., and Graf, G., "Close-Coupled SCR," *CLEERS Conference*, 2021. Style Reference text

Lehtoranta, K., Vesala, H., Koponen, P., and Korhonen, S., "Selective catalytic reduction operation with heavy fuel oil: NO<sub>x</sub>, NH<sub>3</sub>, and particle emissions," *Environmental Science and Technology* 49(7), 2015, doi:10.1021/es506185x.

Lehtoranta, K., Murtonen, T., Vesala, H., Koponen, P., Alanen, J., Simonen, P., Rönkkö, T., Timonen, H., Saarikoski, S., Maunula, T., Kallinen, K., and Korhonen, S., "Natural Gas Engine Emission Reduction by Catalysts," *Emission Control Science and Technology* 3(2), 2017, doi:10.1007/s40825-016-0057-8.

Maunula, T. and Wolff, T., "Durable Copper and Iron SCR Catalysts for Mobile Diesel and Dual-Fuel Applications," *SAE Technical Papers* 2016-October, 2016, doi:10.4271/2016-01-2214.

Maunula, T., Tuikka, M., and Wolff, T., "The Reactions and Role of Ammonia Slip Catalysts in Modern Urea-SCR Systems," *Emission Control Science and Technology* 6(4):390–401, 2020, doi:10.1007/S40825-020-00171-1.

Murtonen, T., Lehtoranta, K., Korhonen, S., Vesala, H., and Koponen, P., "Imitating emission matrix of large natural gas engine opens new possibilities for catalyst studies in engine laboratory," *28th CIMAC World Congress*, 2016.

Seneque, M., Courtois, X., Can, F., and Duprez, D., "Direct Comparison of Urea-SCR and NH<sub>3</sub>-SCR Activities Over Acidic Oxide and Exchanged Zeolite Prototype Powdered Catalysts," *Topics in Catalysis* 59(10–12):938–944, 2016, doi:10.1007/S11244-016-0572-4.